NCAR | NATIONAL CENTER FOR ATMOSPHERIC RESEARCH

Remote Oceanic Meteorology Information Operational (ROMIO) Technology Transfer

Software Release Package Documentation
Scientific Descriptions of the CDO and CTH Products

Author: Cathy Kessinger
NCAR Research Applications Laboratory
Boulder, Colorado

19 August 2021

Table of Contents

List of Figures

List of Tables

Scientific Description of the ROMIO Cloud Top Height (CTH) and Convection Diagnosis Oceanic (CDO) Algorithms

Executive Summary

Key points for the ROMIO Cloud Top Height (CTH) and Convection Diagnosis Oceanic (CDO) algorithms are:

- GOES-16, GOES-17, and Himawari-8 satellites are used, with the domain covering approximately 78°E to 10°W longitude and -50°S to 70°N latitude. Satellite mosaics are created from the full disk scans at 10 min intervals using the latest data available from each satellite.
- The Cloud Top Height (CTH) product displays cloud top contours at flight altitudes of FL320, FL340, FL360, FL380 and FL400 by converting the satellite IR brightness temperature to flight altitude using a numerical model sounding as reference. The product is designed for opaque clouds.
- The Convection Diagnosis Oceanic (CDO) displays hazards associated with the storm updraft, lightning and overshooting tops, using “interest values” between 0-6 to indicate increasing level of intensity. The CDO is calculated from a weighted combination of four inputs where three inputs are derived from satellite data and one input is derived from lightning data. The three satellite-based inputs are weighted equally to the lightning input, showing the importance of the lightning data in detecting regions of convective hazards. A CDO value of 2 is the threshold where convective hazards may be present. Values of 3 and above indicate the presence of lightning and/or overshooting tops.
- The CTH and CDO products should be viewed together to give a full picture of storm structure. The CTH will contour the entire anvil region of the storm, including both the convective and stratiform regions of the storm. Pilots can use the contours to know their distance from a storm at the flight altitude. The CDO will indicate where the hazard levels are most intense near the updraft. In situations where the convective storms have tops below FL320 (i.e., warm rain situations) and also have had lightning within the last 10-30min, then CDO values are $\geq$3 and indicate a strong storm.
- Polygons approximate the storm contours of CTH and CDO. The XML format of the uplinked polygons has a significant reduction in data volume compared to satellite images, and allows an easy uplink to the aircraft with small bandwidth consumption. Temporal differences can exist across satellites as the mosaic is created, leading to discontinuities in the CTH and CDO polygons. The discontinuity may manifest as a “kink” in the polygon outline.
- The CTH and CDO are supplemental products only and their use is for situational awareness and for long range strategic planning at distances beyond the range of the

onboard weather radar. The onboard weather radar is the primary source of information for tactical flight planning and supersedes other information sources in cases of discrepancies.

- An overview of the ROMIO project, informational videos, and access to CTH and CDO gridded and polygon convective hazard products are available at https://ral.ucar.edu/projects/oceanic-convection-diagnosis-and-nowcasting.

Background on the ROMIO demonstration

The Remote Oceanic Meteorological Information Operational (ROMIO) demonstration (Frazier et al., 2018; Kessinger et al. 2020) was conducted to evaluate the feasibility of uplinking convective weather information to the flight deck of aircraft operating over remote, oceanic regions on transoceanic flights. Pilots operating aircraft in these remote regions have limited access to weather products that depict the current conditions through which they are flying. Access to current weather products is expected to improve pilot decision making in strategic route decisions, cabin management and lead to enhanced fuel savings and greenhouse gas reduction as well as enhanced safety for crew and passengers. Figure 1 shows a comparison of the forward-looking view provided by the onboard weather radar (shown as a half-circle) as compared to the view provided by the ROMIO Viewer. ROMIO gave pilots a much broader view of the weather situation along and around the entire flight route.

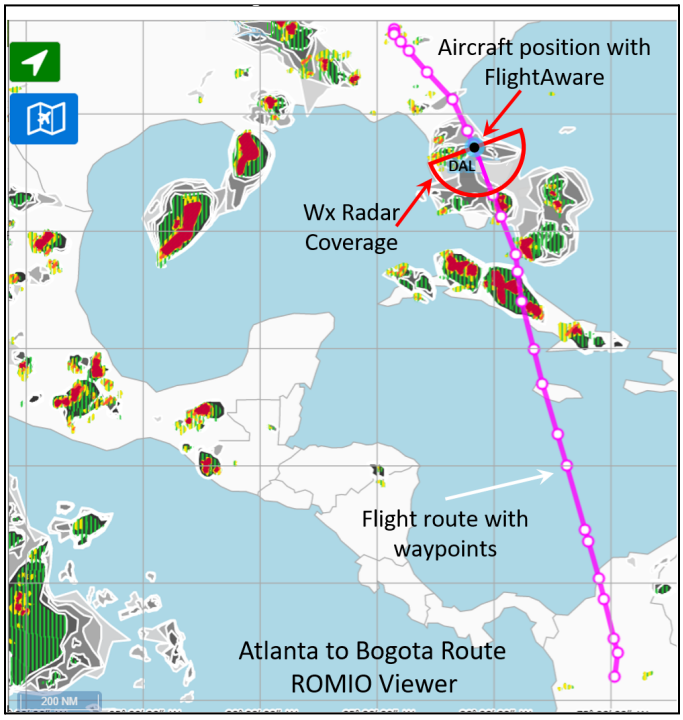

Figure 1. An example of the CTH and CDO products that compares the forward-looking view of the onboard weather radar (red half circle) to the expanded view provided by ROMIO. The planned flight route is shown by the magenta line. The aircraft position was determined with FlightAware locations.

The ROMIO demonstration was conducted from July 2018 to December 2019 and included participants from several agencies. These agencies include the Federal Aviation Administration (FAA) Weather Technology in the Cockpit (WTIC) Program (FAA ANG-C61) acting as sponsor, the National Center for Atmospheric Research (NCAR) acting as principal investigator and overall project support, the Embry-Riddle Aeronautical University providing the NextGen Florida Test Bed, the Basic Commerce and Industries, Inc. (BCI) providing software applications and communications support, three airlines: Delta Air Lines, American Airlines, United Airlines, with Panasonic and Gogo acting as the airlines' datalink-to-aircraft providers and the Virginia Polytechnic Institute and State University (VirginiaTech) providing the benefit analysis. Figure 2 shows the ROMIO system architecture from data ingest and product polygon creation at NCAR, dissemination of the product polygons over the public internet to the Florida Test Bed NAS Enterprise Messaging System (FTB NEMS), then to the BCI Data Management Service (DMS), where the product polygons were then sent to Gogo and Panasonic for transmission to the aircraft over the entertainment wifi network. Product polygons were displayed on tablets using the ROMIO Viewer application (example shown in Figure 1).

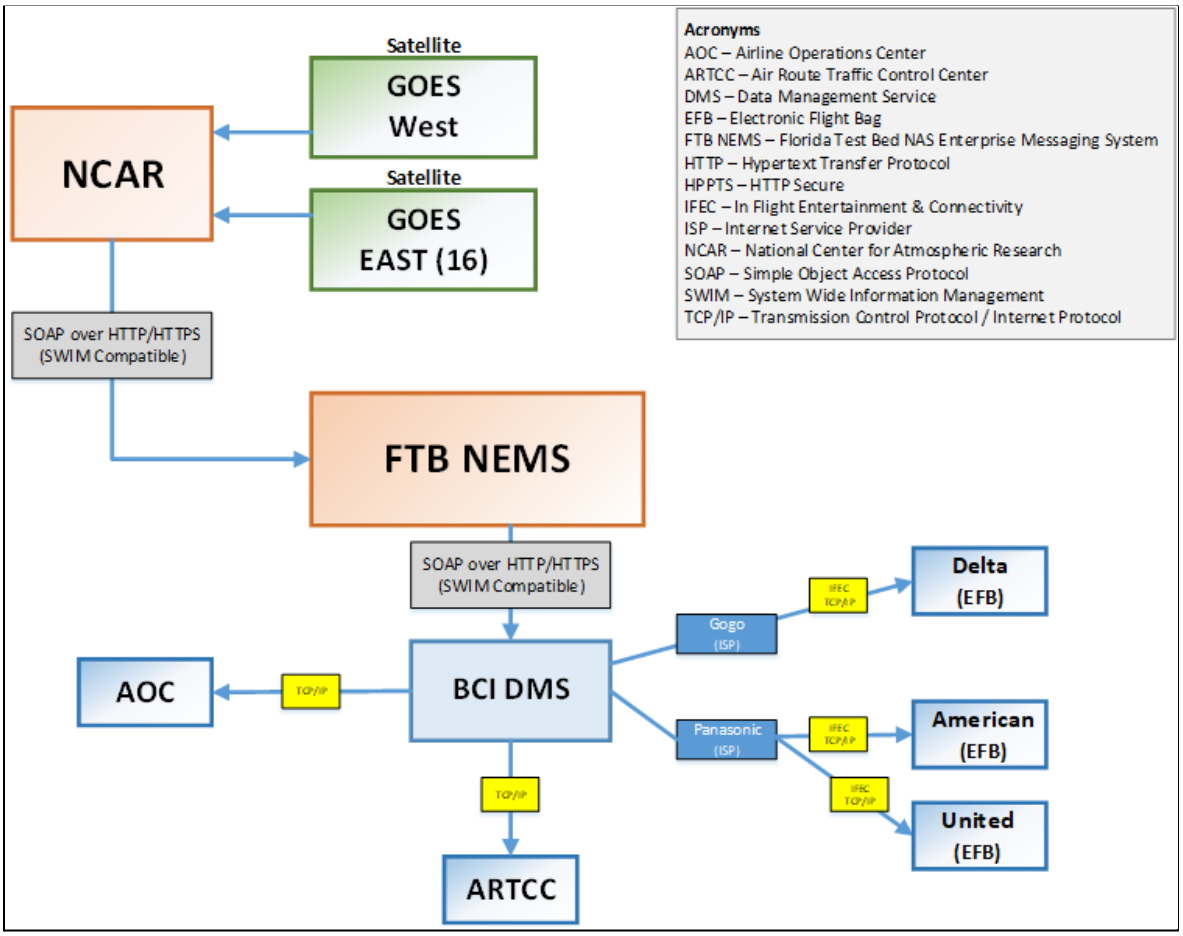

Figure 2. The ROMIO system architecture is illustrated from data ingest at NCAR to final transmission of the CTH and CDO polygons to the airlines, the AOC and to the ARTCC. Note that only the GOES-East and GOES-West satellites were used during the ROMIO demonstration.

The ROMIO demonstration was conducted over the domain covered by the GOES-East and GOES-West satellites (Figure 3). Before and during preparations for the demonstration, the GOES-East and GOES-West satellites were replaced: GOES-13 was replaced with GOES-16 at the GOES-East position and GOES-15 was replaced with GOES-17 at the GOES-West position. These new satellites were a significant technological advancement and allowed an increase in update rate from 15 minutes to 10 minutes and a reduction in temporal and spatial discontinuities because the full disk is now scanned at 10 minute intervals and with a close time-synchronization. In addition, each satellite has the Geostationary Lightning Mapper (GLM) instrument which detects total lightning strikes in remote, oceanic regions with a much higher detection efficiency than ground-based systems can achieve.

After the ROMIO demonstration was concluded, the Japanese Meteorological Agency (JMA) Himwari-8 geostationary satellite was added to the mosaic, leading to an expanded domain that covers much of the Atlantic and Pacific oceans. Following sections discuss the mosaic change in detail.

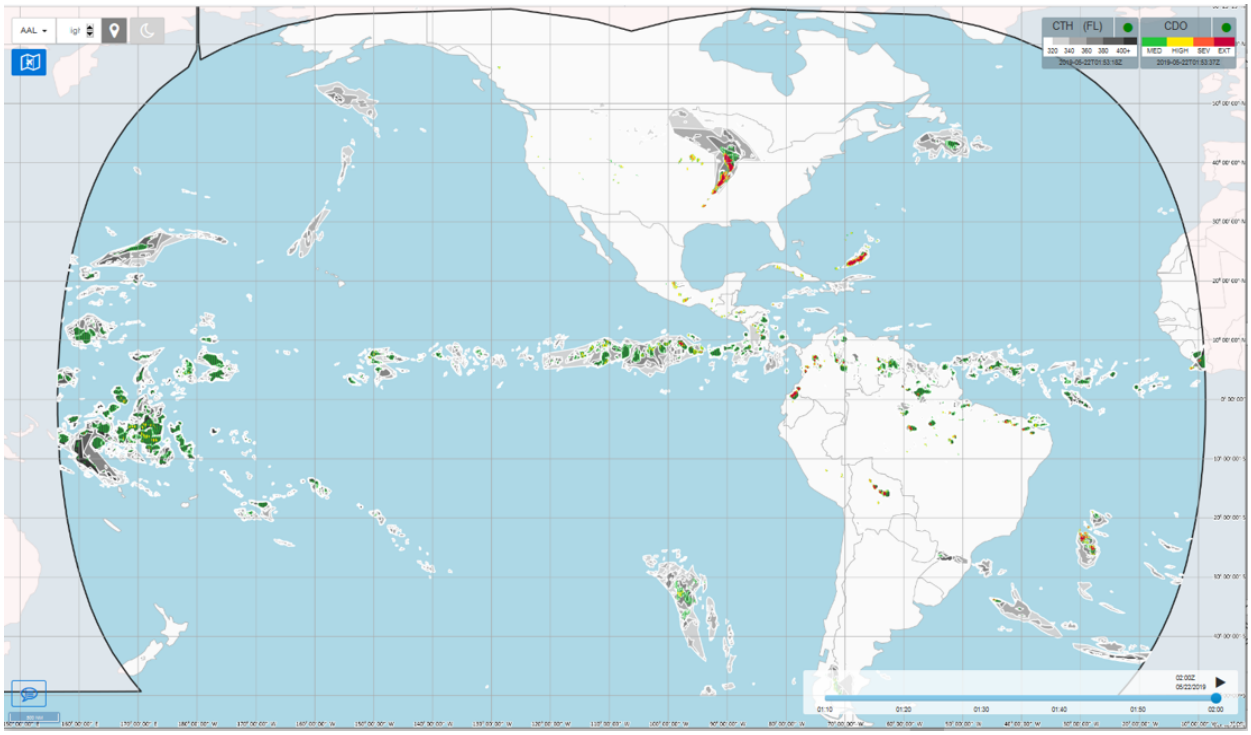

Figure 3. The domain used during the ROMIO demonstration. The scanning areas of GOES-East and GOES-West were used. This image was taken from the ROMIO Viewer developed by BCI.

Examples of the two convective weather products that were uplinked to the flight deck are shown in Figure 4. These products are called the Cloud Top Height (CTH) and the Convection Diagnosis Oceanic (CDO). On the ROMIO Viewer used by pilots, the CTH polygons are shaded in shades of gray at five flight altitudes: FL320, FL340, FL360, FL380, FL400, while the CDO polygons are color-coded by storm intensity. Green means that the storm had a “medium”

intensity, yellow means a “high” intensity, orange means “severe intensity” and red means “extreme intensity”. Color shades of yellow, orange or red mean that the storm updraft is strong enough to produce lightning and/or an overshooting top.

Both algorithms are described in more detail in sections that follow. Briefly, the CTH algorithm converts the satellite infrared brightness temperature to flight altitude using the vertical soundings provided by the NOAA Global Forecast System (GFS) numerical model. The CDO algorithm is a data fusion of three satellite-based algorithms plus ground-based and geostationary lightning strike detections. Once the CTH and CDO products are created on a latitude/longitude grid, specified values are contoured and converted to XML format polygons that can be transmitted to the aircraft with a minimum of communications bandwidth needed. An engineering test of the response bytes per 10 minute update rate used while seven aircraft were using ROMIO shows the CTH used 475-650 Kbytes while CDO used 200-450 Kbytes.

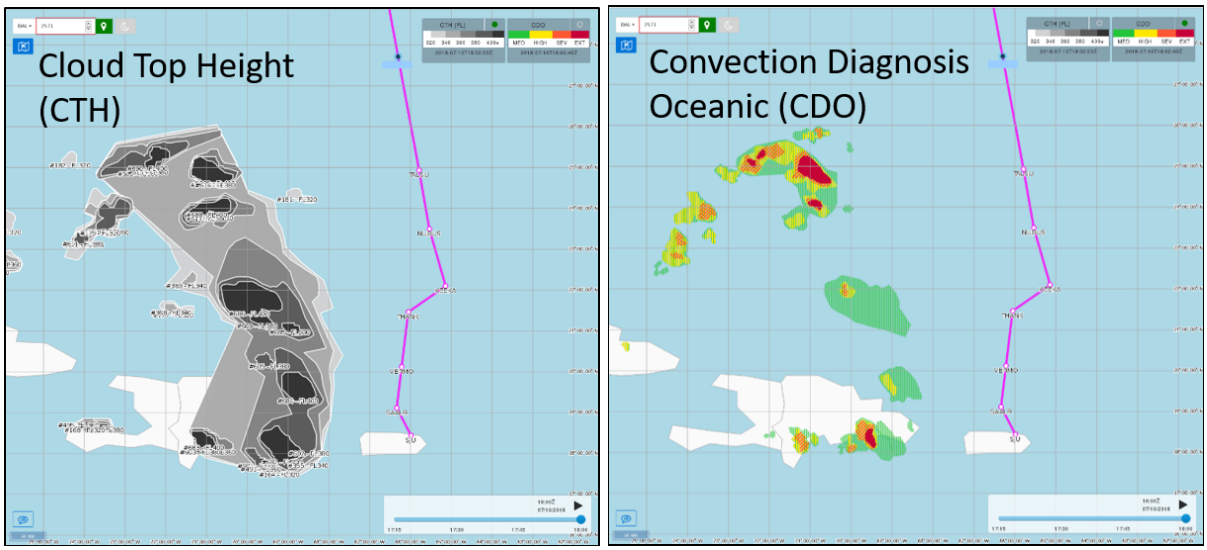

Figure 4. Examples of the CTH (left panel) and the CDO (right panel) products as displayed during ROMIO on the ROMIO Viewer. The planned flight route of an aircraft is shown as the magenta line.

Flight routes flown by the participating airlines were from the CONUS to and from international destinations with particular emphasis desired for flight routes that traversed the Inter-Tropical convergence Zone (ITCZ),a frequent location for convective storms. Each airline determined the aircraft used, routes flown, the number of pilots trained and conducted their pilot training. Delta Air Lines trained 367 pilots that flew the 767-300, the 767-400, 777, A330 and A350 aircraft. United Airlines trained ~10 Line Check Airmen who flew the 777 and 787 aircraft. American Airlines trained ~40 Line Check Airmen who flew the 777-200 aircraft.

The ROMIO demonstration began in July 2018 with Delta Air Lines. United Airlines and American Airlines began participating in spring 2019 as the government shutdown mandated the temporary cessation of the demonstration for several months. The ROMIO demonstration

ended in late December 2019. For a three week period in August-September 2019, there were an average of 26 flights per day using the ROMIO Viewer.

VirginiaTech conducted the benefits analysis to quantify the benefits provided by the ROMIO demonstration, using a multi-step approach (Seo, et al., 2019; Izadi, et al. 2019; Izadi, et al., 2020a; Izadi, et al., 2020b). First, a pilot survey was conducted with 90 usable surveys collected. Of these 90 pilots, 54% of them had a weather deviation on their flight where the average deviation distance was 29 nautical miles, and ranged from 2-120 nautical miles. Second, a statistical data analysis was performed to quantify the types of events and to measure the operational benefits of strategic deviation maneuvers. Lastly, a simulation-based analysis was performed using the Global Oceanic Model.

Findings from the pilot survey are listed below (Seo et al., 2019), and show that ROMIO was successful at demonstrating the benefits of uplinking current weather information into the flight deck.

- **General Workload:** How much effort was required to process information provided by ROMIO compared to current system?
    - 94% of pilots said using ROMIO required the same or less effort
- **Situational Awareness:** How well does ROMIO enable situational awareness in monitoring weather along your flight route in comparison to current system of hardware and procedures?
    - 95% of the pilots perceive equal or improved situational awareness with ROMIO
- **Timeliness:** How well does ROMIO enable obtaining relevant, timely weather information in comparison to current system and hardware?
    - 92% of pilots perceive ROMIO as equal or more effective compared to existing tools
- **Accuracy of CTH and CDO:** How well did ROMIO information correspond to your observation outside the cockpit window? (only for cases where there was an observation)
    - 94.7% of pilots rate ROMIO accuracy between Somewhat to Very Accurate to depict CTH
    - 94.8% of pilots rate ROMIO accuracy between Somewhat to Very Accurate to depict CDO
- **Efficiency and safety:** ROMIO in the context of cabin crew coordination with weather events
    - Most common pilot response: I was able to seat the flight attendants early
        - Enhanced safety of passengers and crew realized

The second stage of the VirginiaTech benefits analysis was to do a statistical analysis of ROMIO flight routes (Izadi et al., 2019). They selected 45 bi-directional origin-destination pairs that are used by the three airlines and selected 18,326 flights for analysis from the FlightAware data base. These flights were conducted during the ROMIO demonstration time period but did not necessarily have a ROMIO Viewer in the cockpit. For these flights, the distances traveled within the CDO contours were measured. They also measured differences attributed to early,

ROMIO-aided strategic deviation decisions due to convective weather. Their study assumed 60 flights crossing the ITCZ per day with 320 operational days per year. Jet fuel was assumed to cost $1.82 per gallon. They analyzed five aircraft types and computed the mean savings, with results shown in Table 1. On average, a flight using ROMIO could see a 12.8 nautical miles savings in travel distance, a 1.6 minute time savings, 355 pound fuel consumption savings and 1110 pound greenhouse gas emissions savings. These are the lower bounds for benefits and represent a significant cost savings of about $1.8 million dollars annually for the airlines.

NO	Aircraft Types	Average Travel Distance Savings (nm)	Average Travel Time Savings (min)	Average Fuel Consumption Savings (lb)	Average Greenhouse Emissions Savings (lb)
1	Airbus A330-300	12.9	1.60	318	992
2	Boeing 767-400	10.1	1.25	230	717
3	Boeing 777-200	12.3	1.50	355	1111
4	Boeing 777-300	13.8	1.80	534	1669
5	Boeing 787-9	14.8	1.85	339	1062
Average		**12.8**	**1.6**	**355**	**1110**

Table 1. Summary of the Virginia Tech benefits analysis for five aircraft types (Izadi et al. 2019). Columns show savings for average travel distance, time, fuel consumption and greenhouse gas emissions by aircraft type and the mean of all aircraft types.

Introduction

In the following sections, the methodology is described that is used to create the satellite mosaics, create the CTH and CDO products, and convert the two products into polygons that can be transmitted to the aircraft. Additional polygons that describe the regions of missing data as well as the maximum CTH value within a CDO≥3 contour are also described.

Creation of the Satellite Mosaic

Overview

Describing a convective cloud using geostationary satellite-based algorithms is challenging as the satellite instruments can only see the outside shell of the convective cloud top and anvil and not within the cloud. To fully characterize the convective cloud so that pilots have a complete understanding of the cloud structure, pilots need to know the maximum altitude attained by the cloud system and where convective hazards associated with the strong updrafts/downdrafts are located to ensure safe avoidance.

To characterize the convective cloud for these purposes, two sets of algorithms are used. First, the Cloud Top Height (CTH) algorithm describes the height contours of the convective clouds

and is used by pilots to estimate distance from the storm contour at altitude and/or to know if it is possible to safely fly over the clouds. Second, the Convection Diagnosis Oceanic (CDO) algorithm detects the region of convective hazards. Separating the region of convective hazards from the stratiform region is less exact using satellite-based algorithms than methodologies utilized with ground-based radars. However, including a ground-based lightning detection network and the GOES-16 and GOES-17 Geostationary Lightning Mappers (GLM) improves the ability of the detection algorithm to define the region of convective hazards caused by updrafts/ downdrafts. A detection algorithm for overshooting tops is also utilized as an indicator for the updraft location; however, overshooting tops are a transient feature and can be missed between update intervals from the satellites.

The coverage of the NOAA GOES-16/East and GOES-17/West satellites and the JMA Himawari-8 satellites defines the expanded ROMIO demonstration domain (Fig. 5) that is currently available. Note that much of the Atlantic and Pacific oceans are covered with this revised and expanded domain. Realtime data are freely available from the Amazon S3 service for all three satellites. Access to these data are described in the companion report that describes the ROMIO CTH/CDO system.

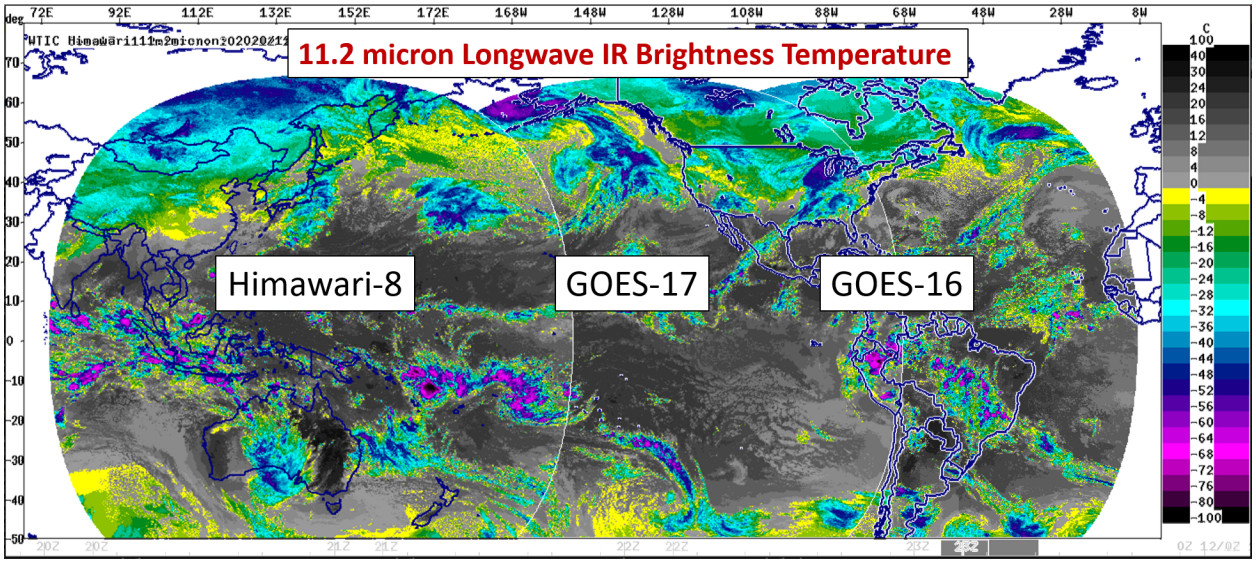

Figure 5. The ROMIO domain is shown and contains three satellites: Himawari-8, GOES-17 and GOES-16. The 11.2 micron brightness temperature is shown. Data have been overlaid and not mosaicked.

All three satellites were launched with new, state-of-the-art instruments called the Advanced Baseline Imager (ABI) for the GOES satellites and the Advanced Himawari Imager (AHI) for the Himawari-8 satellite. These new satellite imagers represent a significant advance in capability over previous satellites. All scan the full hemisphere (i.e., also called full disk) at 10 minute intervals.

The GOES-17 satellite was successfully launched and placed into orbit in 2018. However, problems with the ABI were discovered during system check-out. Initially, the cooling system had a malfunction that prevented full operation of all the channels, notably the infrared channels

used by ROMIO. The ABI instrument would overheat when the sun was shining on it, degrading performance and compromising data quality. The result was that these channels would be available only for 12 hrs/day and only during daylight hours. A team of experts made changes to the flight configuration of the satellite such that the infrared channels are now available for all but 2-6 hrs during the night, depending on wavelength and day of the year. An adjustment was made to the CDO algorithm during times when the water vapor channel is not available. The 11.2 micron channel is no longer significantly impacted.

For GOES-16 and GOES-17, a new instrument, called the Geostationary Lightning Mapper (GLM), is providing total lighting flashes (i.e., cloud-to-ground, cloud-to-cloud, and/or in-cloud flashes) between the latitude limits of -52 S and 52 N. The GLM data are combined with the ground-based lightning network to provide detailed information on convective hazards. The GLM and ground-based lightning network are both being utilized within the CDO product.

Scanning strategies

Each of the satellites in the ROMIO domain perform full disk scans at 10 minute intervals. GOES-16 and GOES-17 are synchronized such that their full disk scans begin and end times are 10-15 secs apart. The Himawari-8 satellite is nearly synchronized with the two GOES satellites with start and end times occurring within ~30 sec of the GOES satellites. This synchronization reduces temporal discontinuities across satellites, assuming all data input into the mosaic are current for a given time.

From the time the satellite scan ends, the latency before GOES data are available for ingest by the ROMIO processing system is about 1 minute. The latency for Himawari-8 data is about 4 minutes.

Mosaic creation

For the ROMIO processing system, the 3-satellite mosaic is created every 10 minutes, using the latest data from each satellite. Figure 6a shows the overlap regions between each satellite. In the overlap region, the data from each satellite are weighted and averaged, using the satellite zenith angle to determine the weight. This process reduces data discontinuities between satellites. However, if the data from one satellite is delayed and the temporal difference is greater than 10 minutes, the CTH and CDO polygons may have discontinuities at the boundaries between satellites. A kink in the polygons may be observed. Figure 6b and 6c show the CTH field from each individual satellite and then the mosaicked CTH field, respectively.

Both the CTH and the CDO will have the same latencies with the satellite-based inputs. However, the CDO product uses a combination of satellite-based algorithms and lightning accumulations to determine convective intensity. The CDO uses ground-based lightning accumulations at 10, 30 and 60 minutes as inputs with the time stamp on the lightning accumulations at the end time. The GLM data only use an accumulation period of 10 minutes. The latency of ground-based lightning data is typically about 2 minutes. The latency of the GLM

data is about 20 seconds. When CDO is ≥3 then lightning is present within the past 10-30 minutes of the time stamp shown on the mosaic.

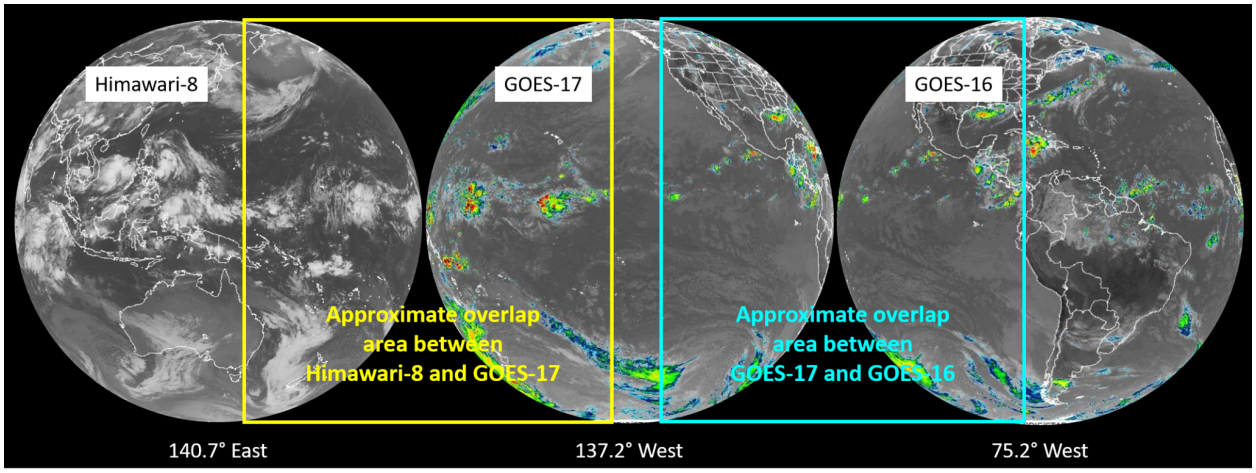

Figure 6a. In the top panel, the area of each satellite's full disk scan is shown for Himawari-8 (left), GOES-West (center) and GOES-East (right). Areas of overlap between satellites are shown with the yellow and cyan boxes.

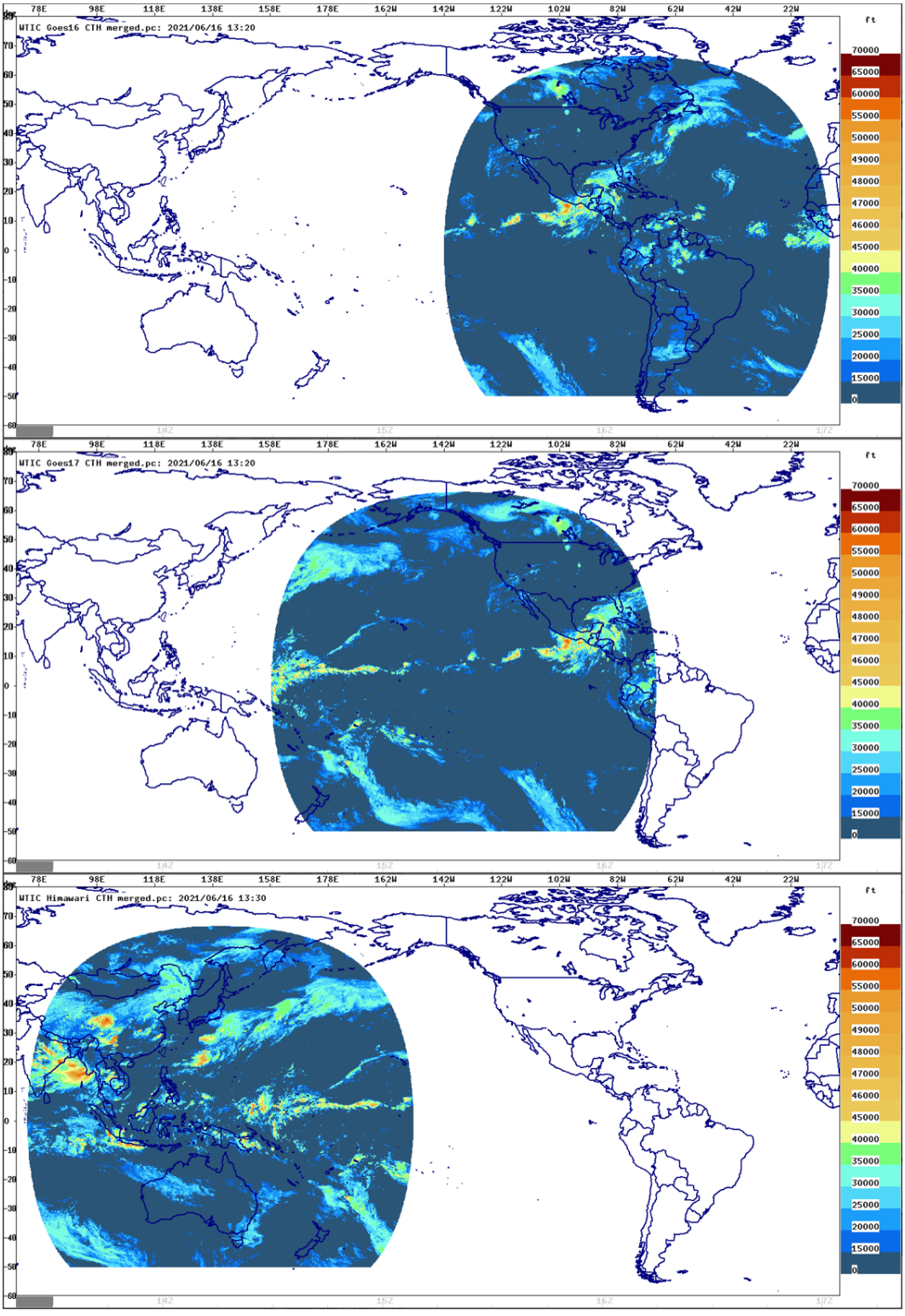

Figure 6b. The CTH fields are shown from each satellite (GOES-East, top; GOES-West, middle; Himawari-8, bottom) before the mosaic is created.

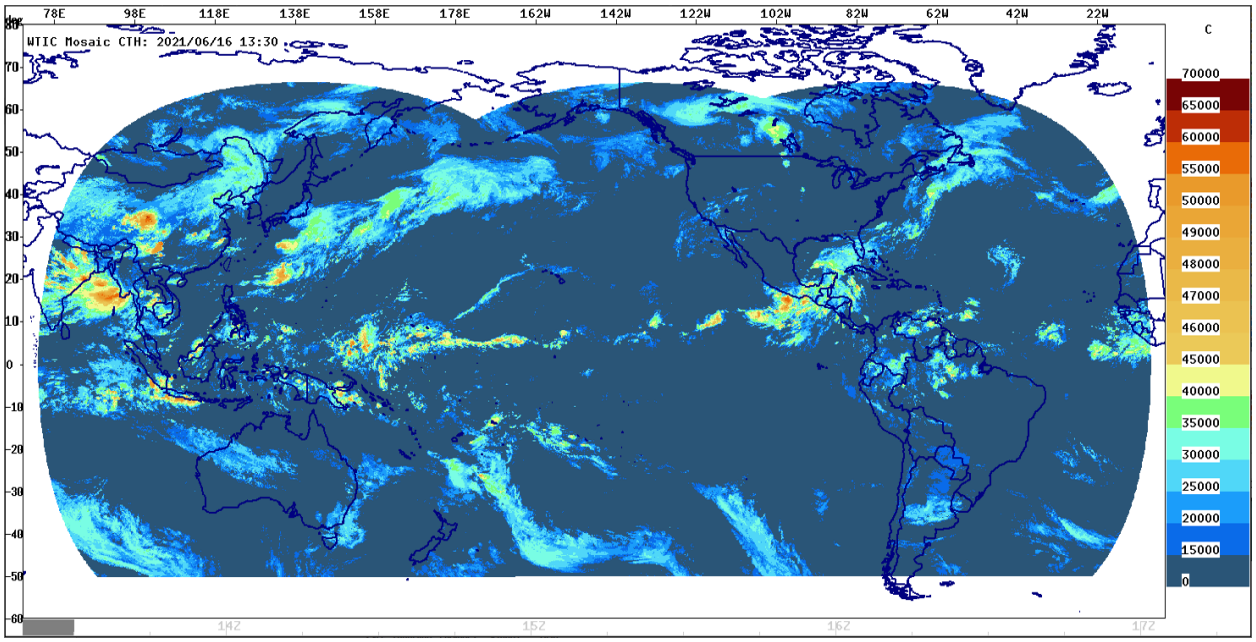

Figure 6c. The final mosaic of the CTH product is shown. Note the smooth transition in values between satellites with no apparent discontinuities observed.

Cloud Top Height (CTH) Algorithm Description

The CTH algorithm (Miller et al. 2005, Donovan et al. 2008) converts the satellite infrared (IR) brightness temperature from the 11.2 micron channel to a flight altitude. The brightness temperature is compared to the atmospheric temperature of the NOAA GFS numerical model to find a matching temperature and determines the pressure level of the IR brightness temperature. Using the standard atmosphere equation, the pressure is converted to flight level. Figure 7 shows the NEXRAD radar reflectivity for a storm complex near the Texas coast for comparison to the CTH and the CDO fields. Figure 8 shows the corresponding IR brightness temperature (left panel) and the computed CTH values (right) for the same day and time.

The CTH algorithm works for both day and night conditions. It is designed to perform best for opaque clouds, like deep convection. The IR brightness temperatures of thin cirrus clouds are typically contaminated by the warmer surface temperature with the result that their computed heights are too low, which improves their elimination as convective clouds. Cloud top heights below FL150 are not computed by the algorithm. The CTH field can be computed globally as all satellites have this channel available. Figure 9 shows an example of the CTH calculated over the ROMIO domain, for a different day.

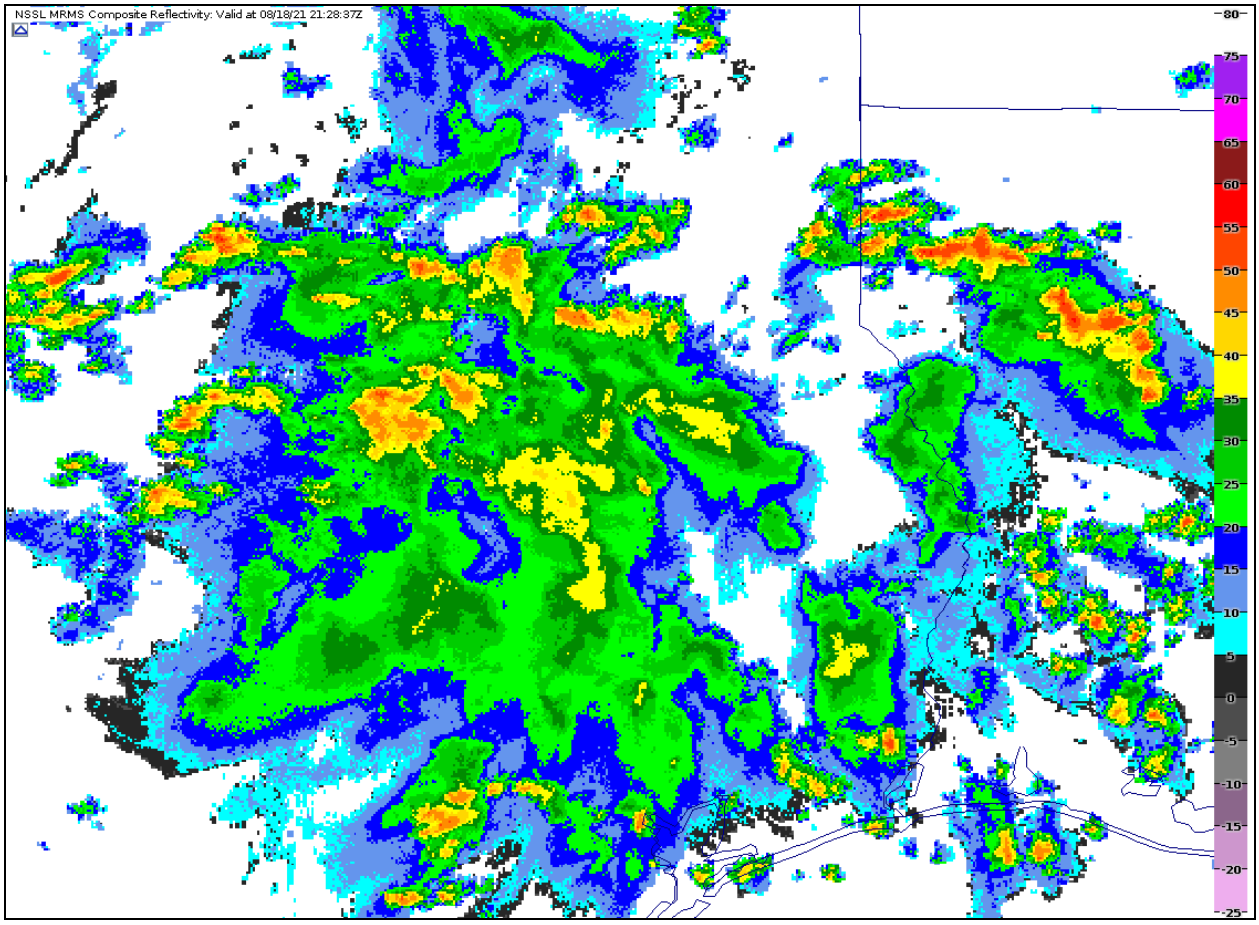

Figure 7. An example of NEXRAD reflectivity is shown for storms near the Texas coast for comparison to CTH and CDO.

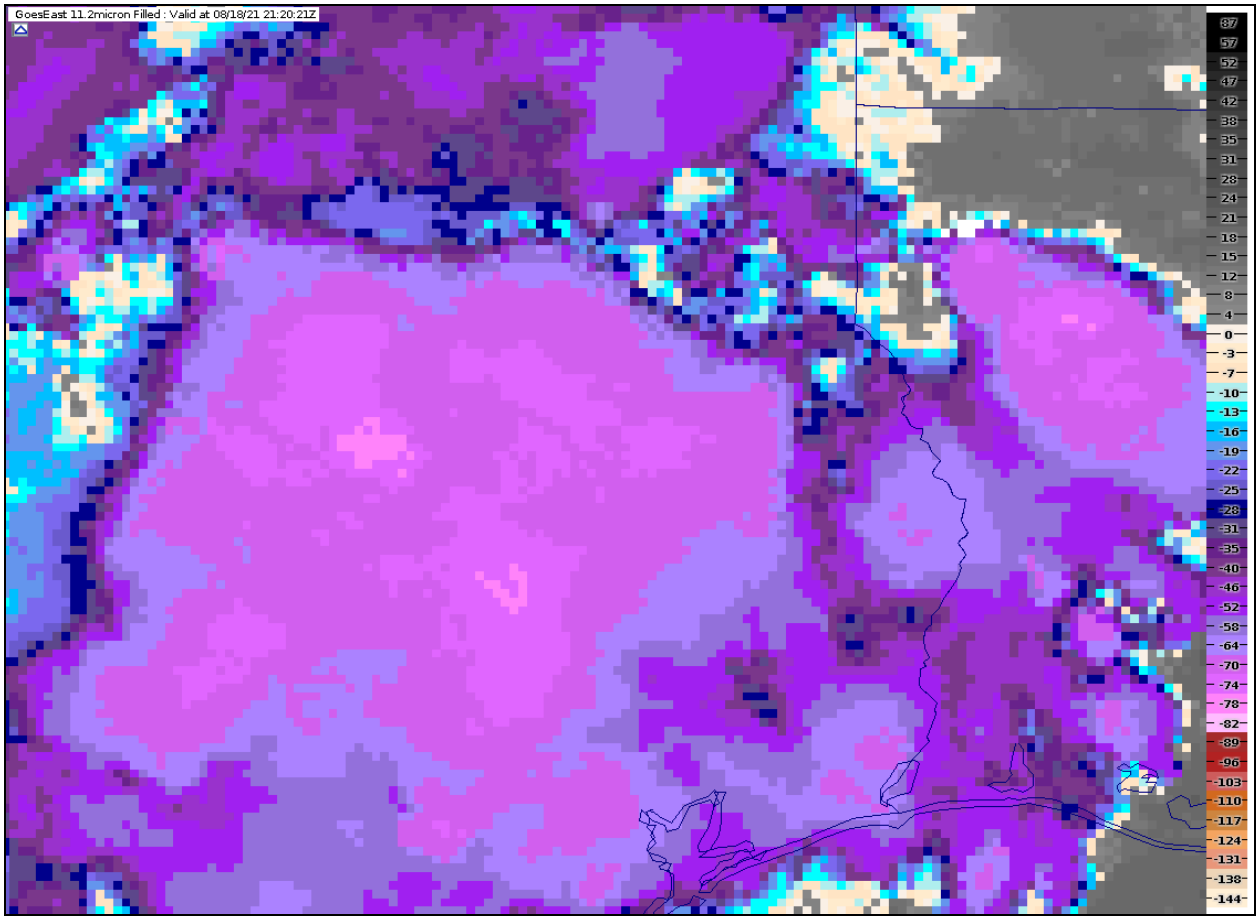

Figure 8a. An example of IR brightness temperature. Figure continues below.

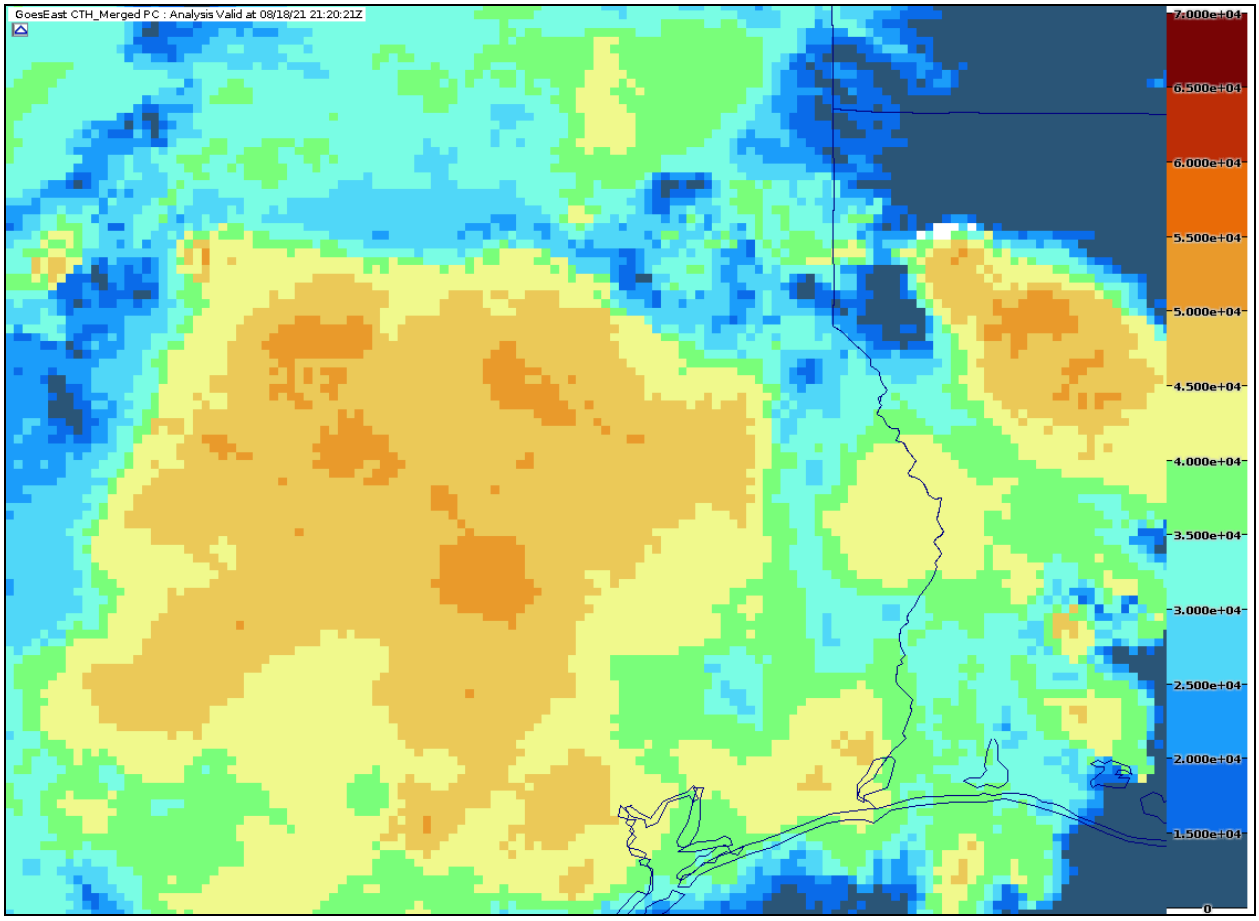

Figure 8b. The corresponding Cloud Top Height (CTH) field derived from the IR brightness temperature shown in Figure 8a.

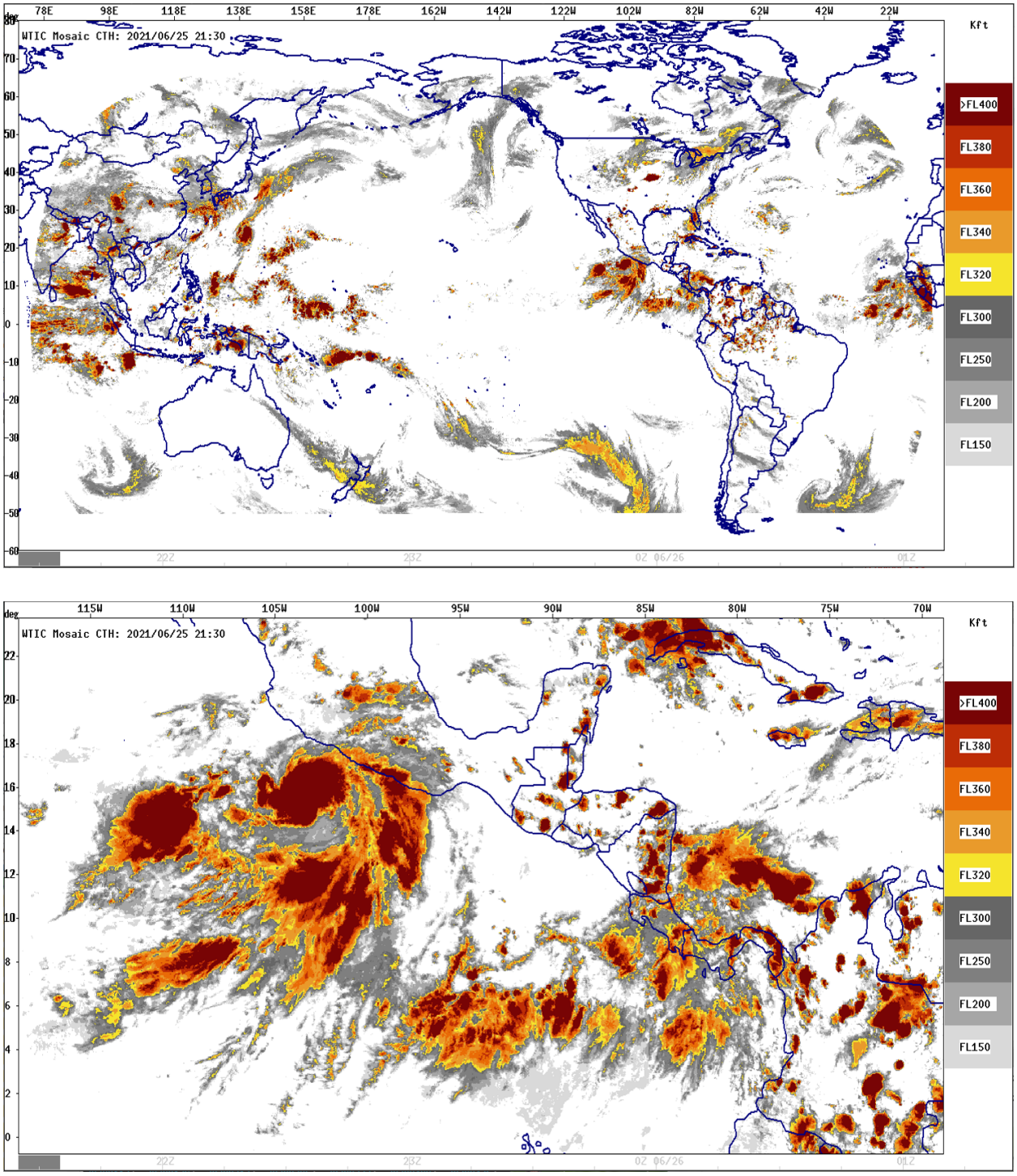

Figure 9. The CTH field is computed over the ROMIO domain (not the same day as shown in Figures 7-8). The CTH contours are FL320 (yellow) through shades of orange to FL400 and above (brown). Flight levels at and below FL300 are shown in shades of gray. The top panel shows CTH as computed over the entire ROMIO domain and the bottom panel shows CTH over Central America. The date is 25 June 2021 at 2130 UTC for both.

Lightning Strike Data

To provide full coverage of lightning data over the ROMIO 3-satellite domain, data from a ground-based global lightning detection network are merged with total lightning data from the two Geostationary Lightning Mapper (GLM) instruments that are onboard the GOES-East and GOES-West satellites (Figure 10).The ground-based network provides full coverage over the entire domain while the geostationary instruments are not available over the entire ROMIO domain. Merging the data from the two systems maximizes the area where lightning is detected.

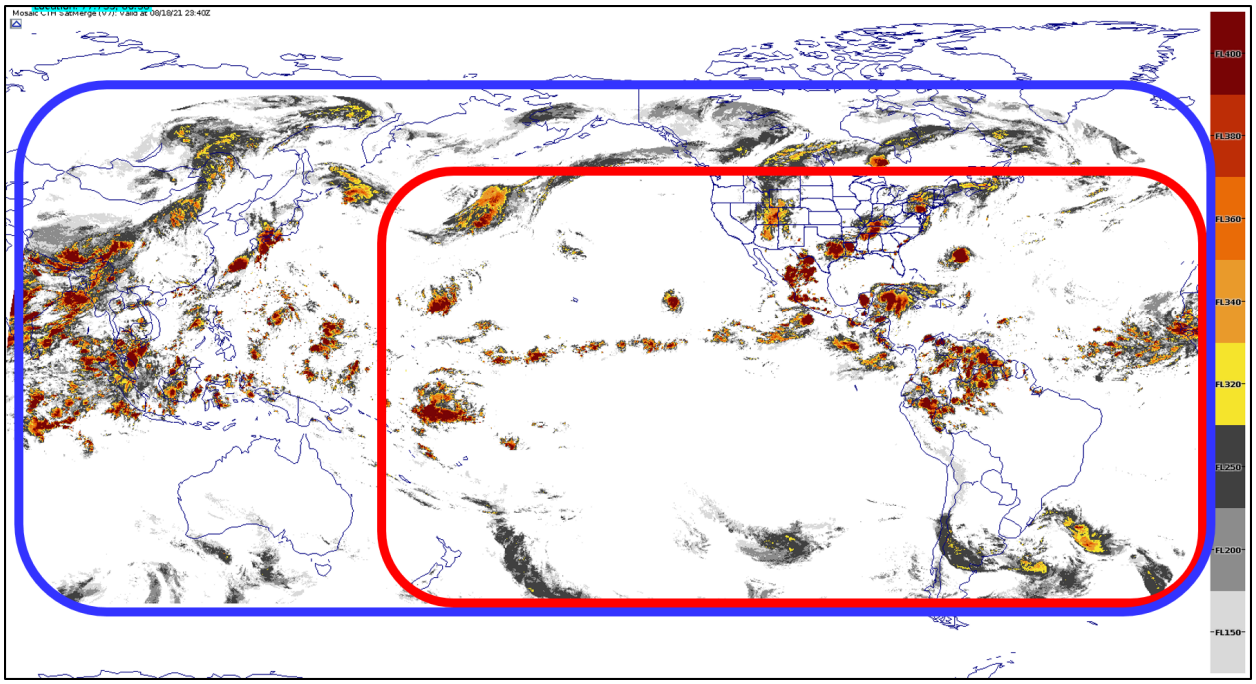

Figure 10. Panel shows the area where GLM data from GOES-16 and GOES-17 are available within the ROMIO domain (red polygon). Ground-based lightning data are available within the entire ROMIO domain (blue polygon). Cloud Height Top data are shaded.

The GOES-East and GOES-West GLM instruments provide total lightning data with detection of cloud-to-ground and cloud-to-cloud strikes. These data will provide much improved detection of lightning location, particularly in the remote oceanic regions, where ground-based detection networks have low detection efficiency. The GLM operates between -52° S and 52° N latitude (Figure 10). The GLM data files are produced every 20 seconds and have a 20 second data latency. The GLM data will be used within the CDO product; however, because regions outside of the GLM domain will not have GLM data, there must be a merging of the ground-based lightning network and GLM datasets. To ensure that the CDO product has the same look-and-feel across the entire ROMIO domain, the GLM accumulations use an accumulation period of 10 minutes only.

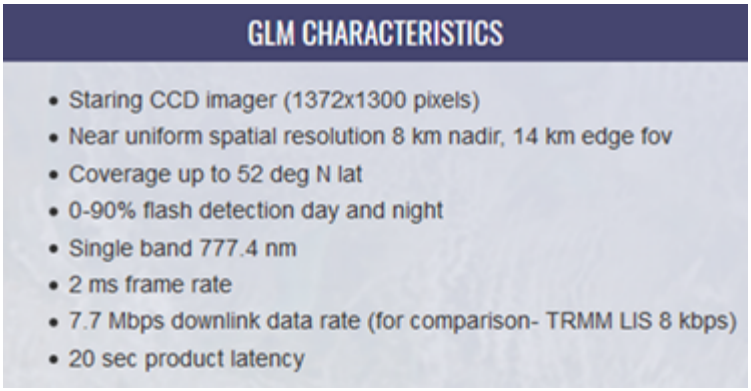

Figure 11. Characteristics of the GOES-16 and GOES-17 Geostationary Lightning Mapper (GLM). Provided by courtesy of the NOAA GOES-R web site at (http://www.noaa.gov/goesR).

A ground-based lightning detection data set is needed to provide lightning coverage in regions where the GLM data do not exist. Data are provided by a number of vendors and it is the user's responsibility to acquire these data for ingest into the ROMIO processing system. Typically, ground-based detection of lightning strikes includes the location and time of each strike. These data typically are available at one minute intervals where each file contains one minute of data. Typically, about a 2 min latency of the data files is observed. Once received, strike accumulations are computed where the strike locations are gridded to the nearest grid point and a count is incremented. Strike accumulations are computed at 10, 30 and 60 minute intervals that are updated at 10 min intervals. The accumulations are computed in this manner because ground-based lightning detection has a low efficiency in the remote oceanic regions. The 10 minute interval is chosen because storms producing recent lightning are the most hazardous and because 10 minutes is the update interval for the ROMIO system. The 30 minute interval is chosen because that is a "typical" life time of many convective cells and hazards are likely present as the storm reaches maturity and begins dissipating. The 60 minute interval gives a margin of aviation safety for dissipating storms and for storms in remote regions where the lightning detection efficiency is low. Additional processing of the lightning strike accumulation files are described below in the CDO section.

Convection Diagnosis Oceanic (CDO) Algorithm Description

The CDO algorithm (Kessinger et al. 2017; Donovan et al. 2009) is used to detect the area of storms that are most hazardous for aviation by combining geostationary satellite-based algorithms and ground-based lightning detection data in a fuzzy logic, data fusion methodology. These two contributions to CDO have equal weight, thus illustrating the importance of lightning data in detecting hazardous regions of convection. The inputs to CDO are scaled using membership functions that are stepwise linear and that scale the input data to be between zero and unity. As values approach unity, a positive indicator for the presence of a convective hazard is attained. The output is termed an "interest field" or a "likelihood field." The interest fields are weighted and summed, but not normalized. The maximum value of CDO is six with values $\geq$3 indicating lightning and/or an overshooting top is present. Figure 12 shows an overview of the CDO algorithm and all computational steps.

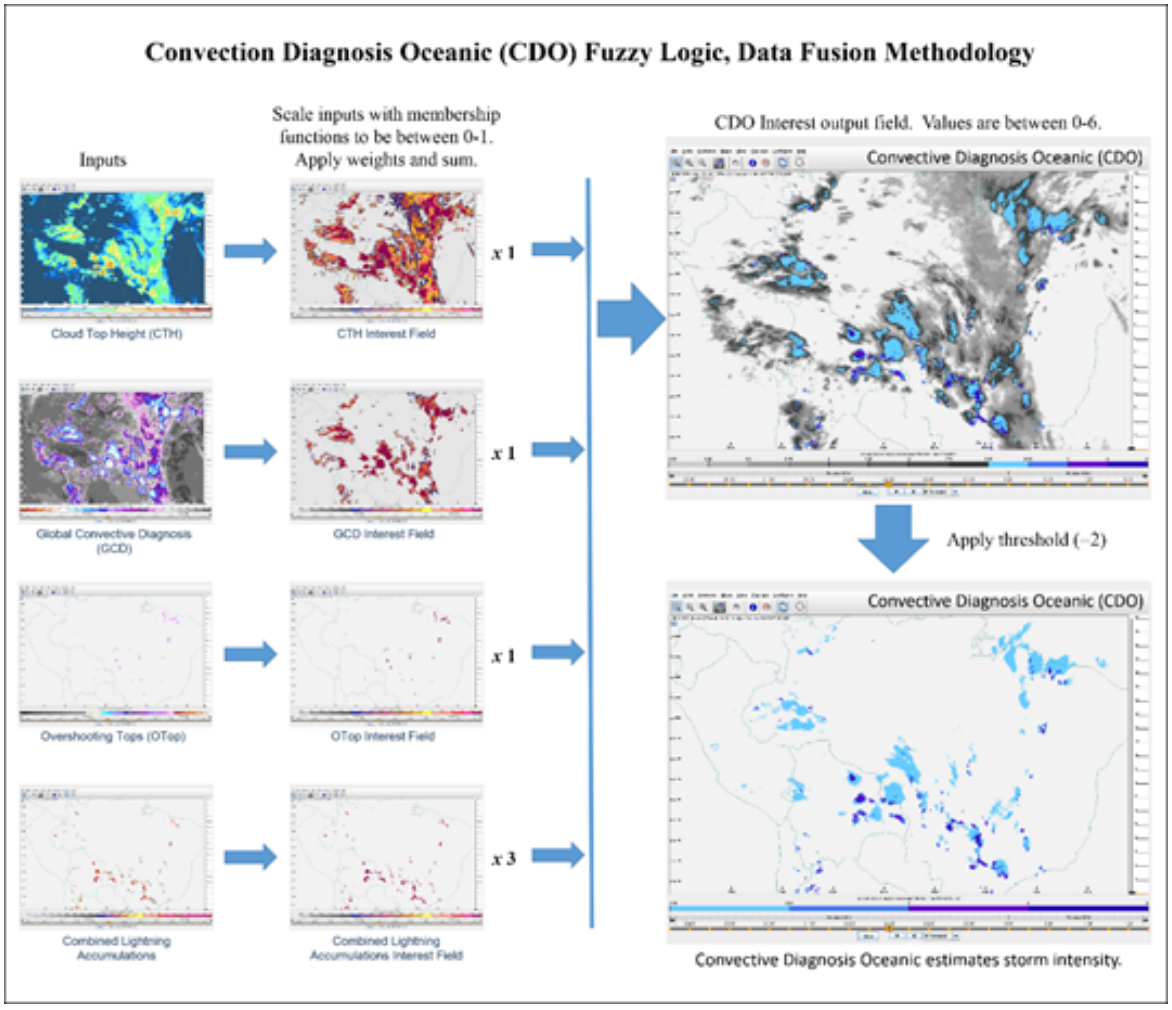

Figure 12. A schematic showing the steps for calculation of the CDO algorithm (Kessinger et al., 2017).

The CDO input fields are the CTH, the Global Convection Diagnosis (GCD; Mosher, 2002), the GOES-R Overshooting Tops Detection algorithm (OTops; Bedka et al. 2010) and a combined lightning field that includes both ground-based and geostationary lightning strike accumulations. An example of each is shown in Figure 13.

The CTH algorithm was described above and is also shown in Figure 13a. The membership function scales the CTH values to vary linearly between FL164 (interest = zero) and ≥FL400 (interest = unity). The weight applied to the CTH interest field is unity.

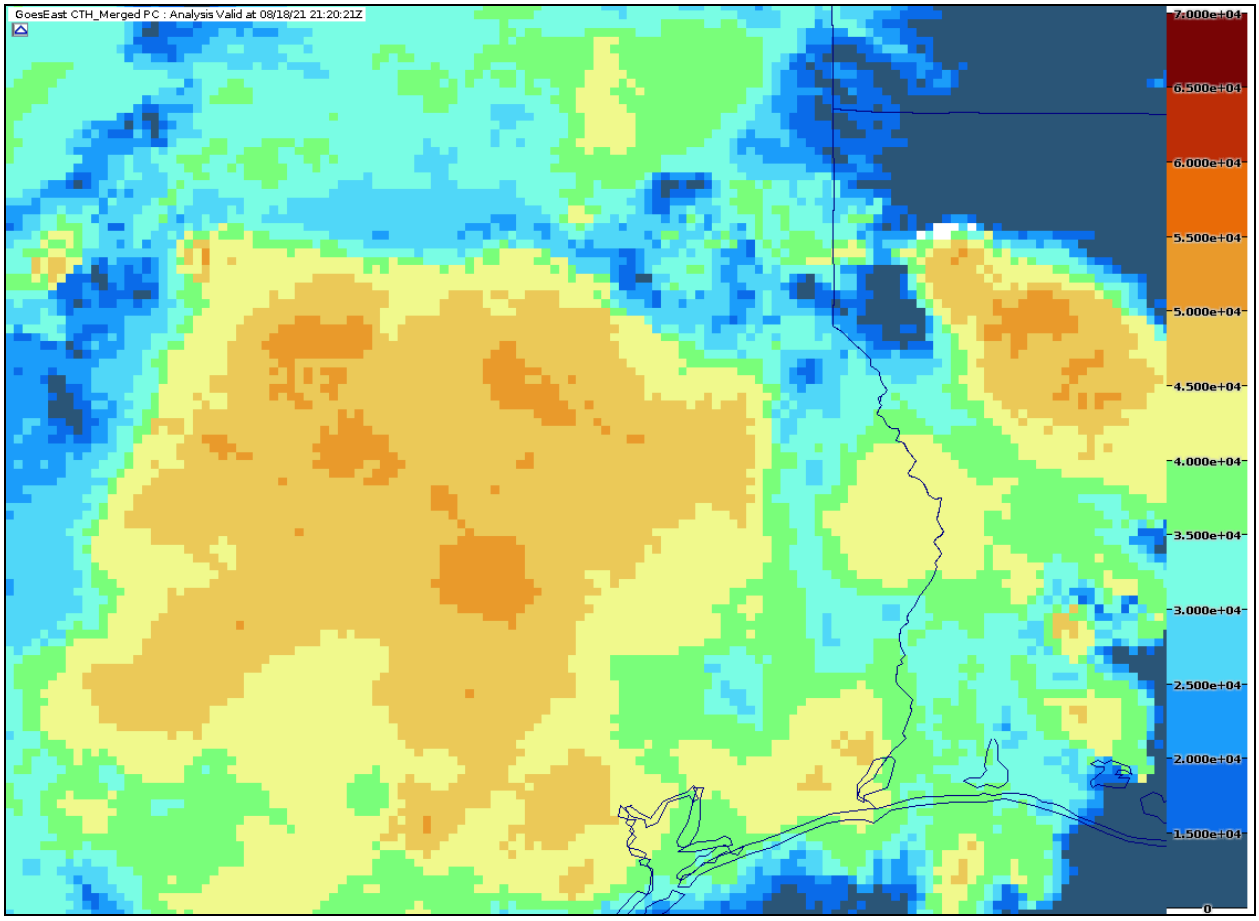

Figure 13a. The CTH field is shown. Figure continues next page.

The GCD algorithm (Figure 13b) uses a channel difference where the IR (11 micron) brightness temperature is subtracted from the water vapor (6.7 micron) brightness temperature. Values near zero indicate the presence of a mature updraft. The membership function scales the GCD interest values to be unity for difference values ≥-0.68°C. The weight applied to the GCD interest field is unity.

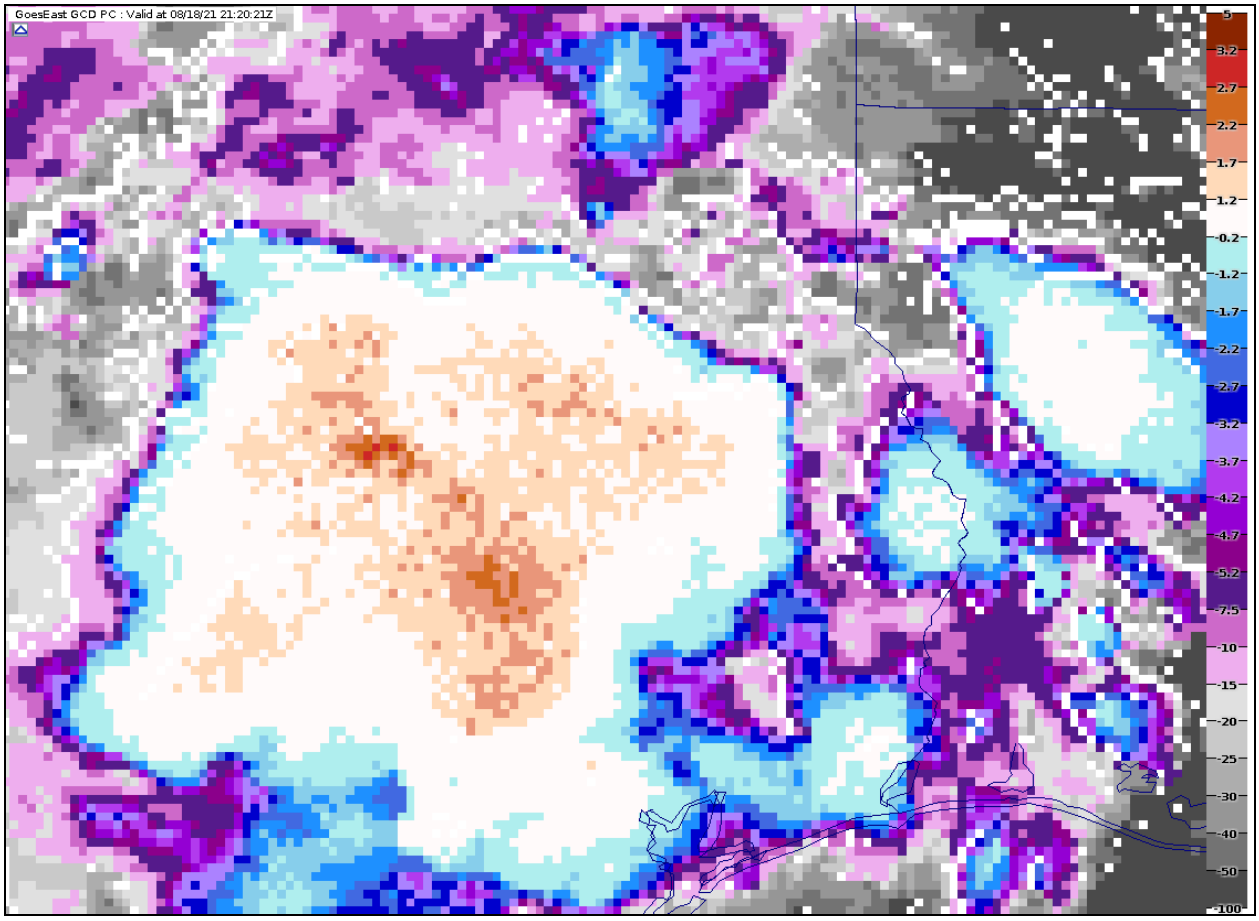

Figure 13b. The GCD is shown. Figure continues below.

The OverShooting Tops Detection (OTops) algorithm (Figure 13c) produces a brightness temperature field where there is a positive indicator for the presence of overshooting tops. The membership function scales the OTops brightness temperatures to unity for all values. The weight applied to the OTops interest field is unity.

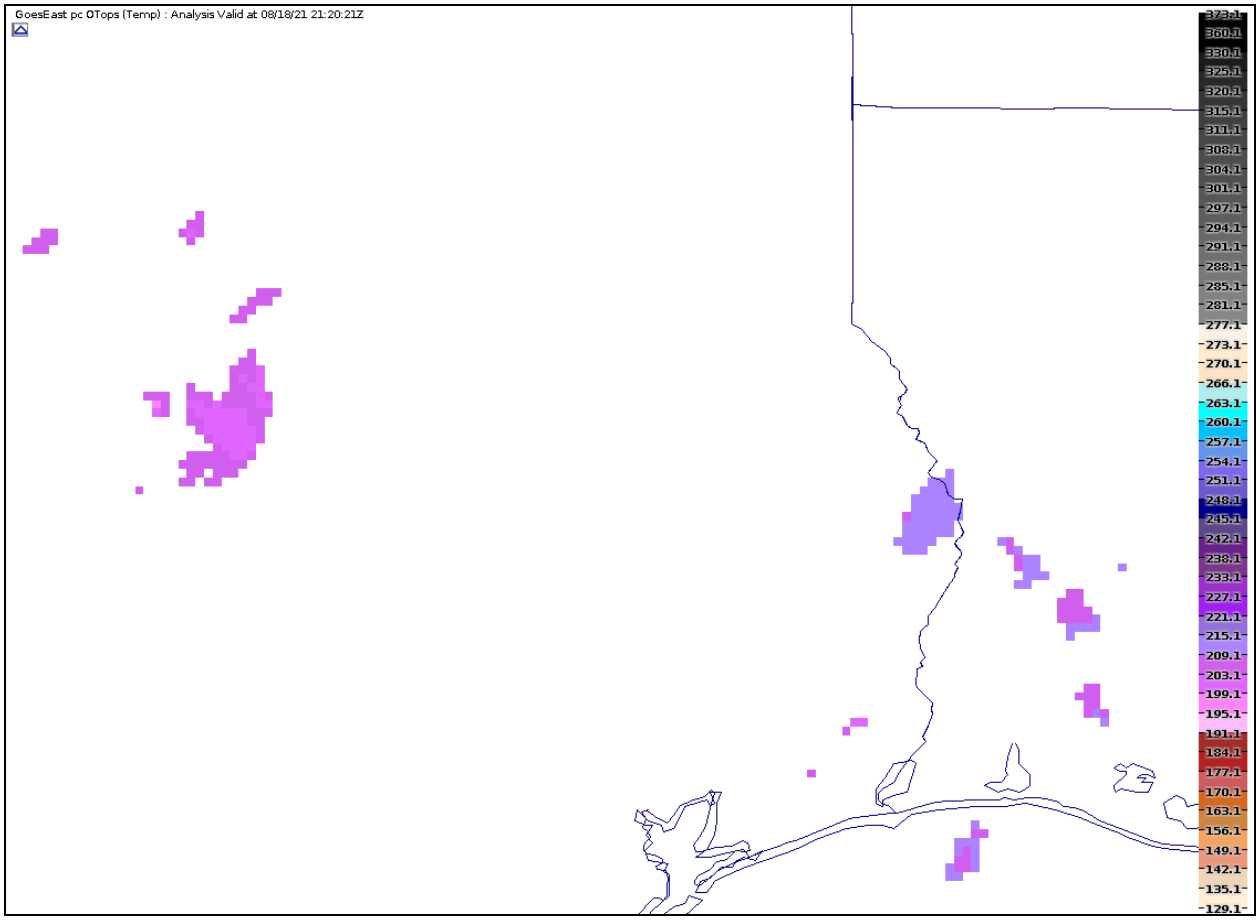

Figure 13c. The OTops algorithm output is shown. Figure continues next page.

The geostationary and ground-based lightning detection data are utilized via a two-step process within the CDO algorithm. As described above and prior to input into CDO, the first step is to compute ground-based lightning strike accumulation fields at three intervals: 10, 30 and 60 minutes. The geostationary lightning accumulation is done for a 10 minute interval. Each of these accumulation fields are combined in a fuzzy logic scheme where each accumulation period has a maximum value of one for any strikes >1. The maximum interest value within the combined lightning interest field is three. Figure 13d shows an example of the combined lightning accumulation field. The field produced by this combination of accumulation fields is then used as an input into the CDO algorithm where the membership function scales all input values $\geq$2 to unity. The weight applied in the CDO calculation for the combined lightning field is three. Because lightning gives the clearest signal that a convective hazard is present, this field is weighted the same as the combination of the three satellite-based algorithms.

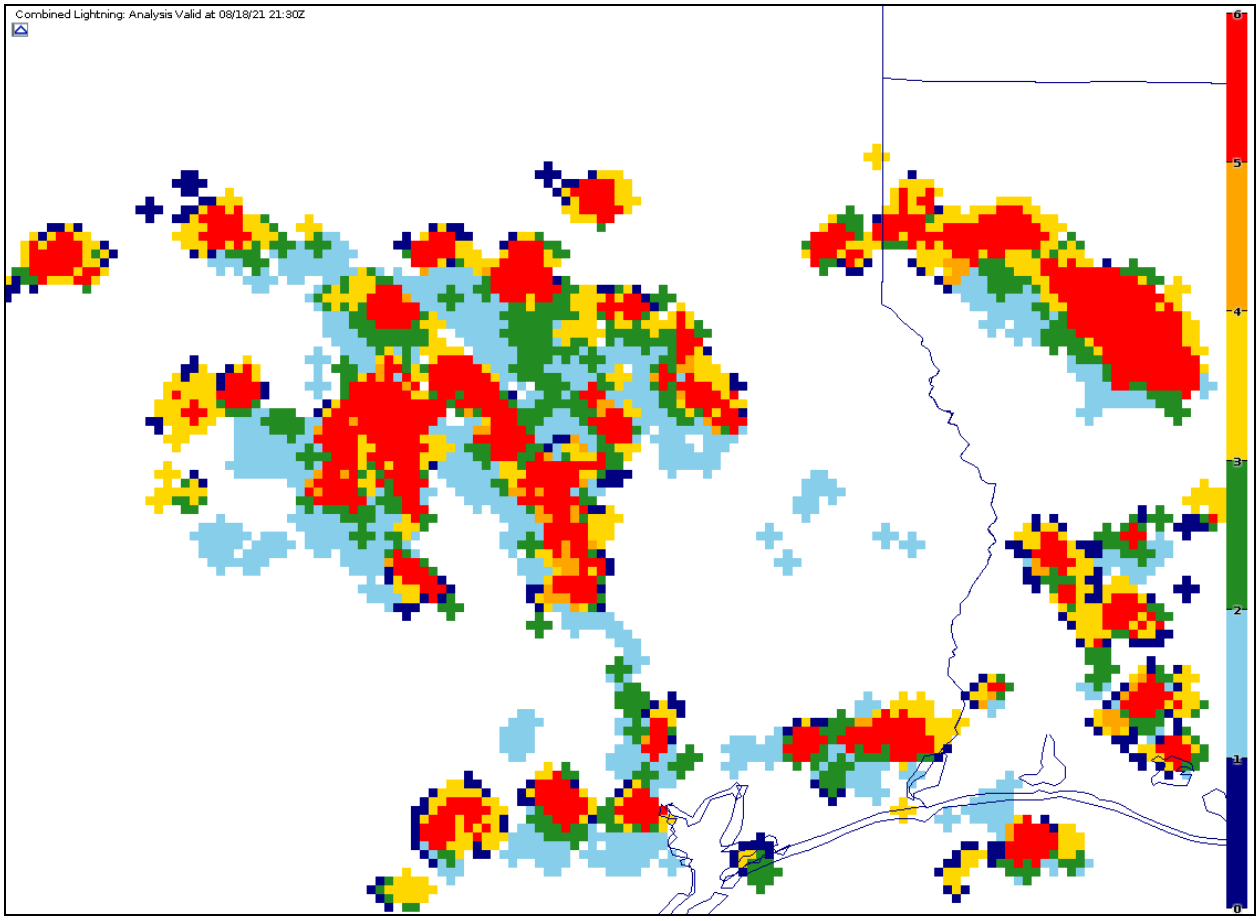

Figure 13d. The Combined Lightning interest field is shown.

Using three accumulation periods for ground-based lightning detection strikes allows the developing, mature and dissipating stages of the convection to be better resolved in remote regions where lightning detection efficiency is low. For developing and mature storms, all three accumulations will contribute to the combined lightning interest field and should yield close to the maximum interest value and a high CDO value ($\geq$3). For dissipating storms, it is likely that only the 60 minute accumulation will contribute. As described above, the GOES-East and GOES-West GLM data are added to the lightning accumulation field within the 10 minute accumulation period.

Once the four input fields are scaled and weighted, the final CDO output (Figure 14) is a summation of the weighted inputs. The CDO varies between zero and six in value. Typically, if only the CTH and GCD are contributing to the CDO interest (most common situation for oceanic convective storms where lightning frequency is lower than that observed for continental storms), the maximum CDO interest values will be two. Once lightning is present or an overshooting top is detected, the CDO values increase to be between three and six and the intensity of convective hazards increases. The CDO field is shown in Figure 15 over the ROMIO domain.

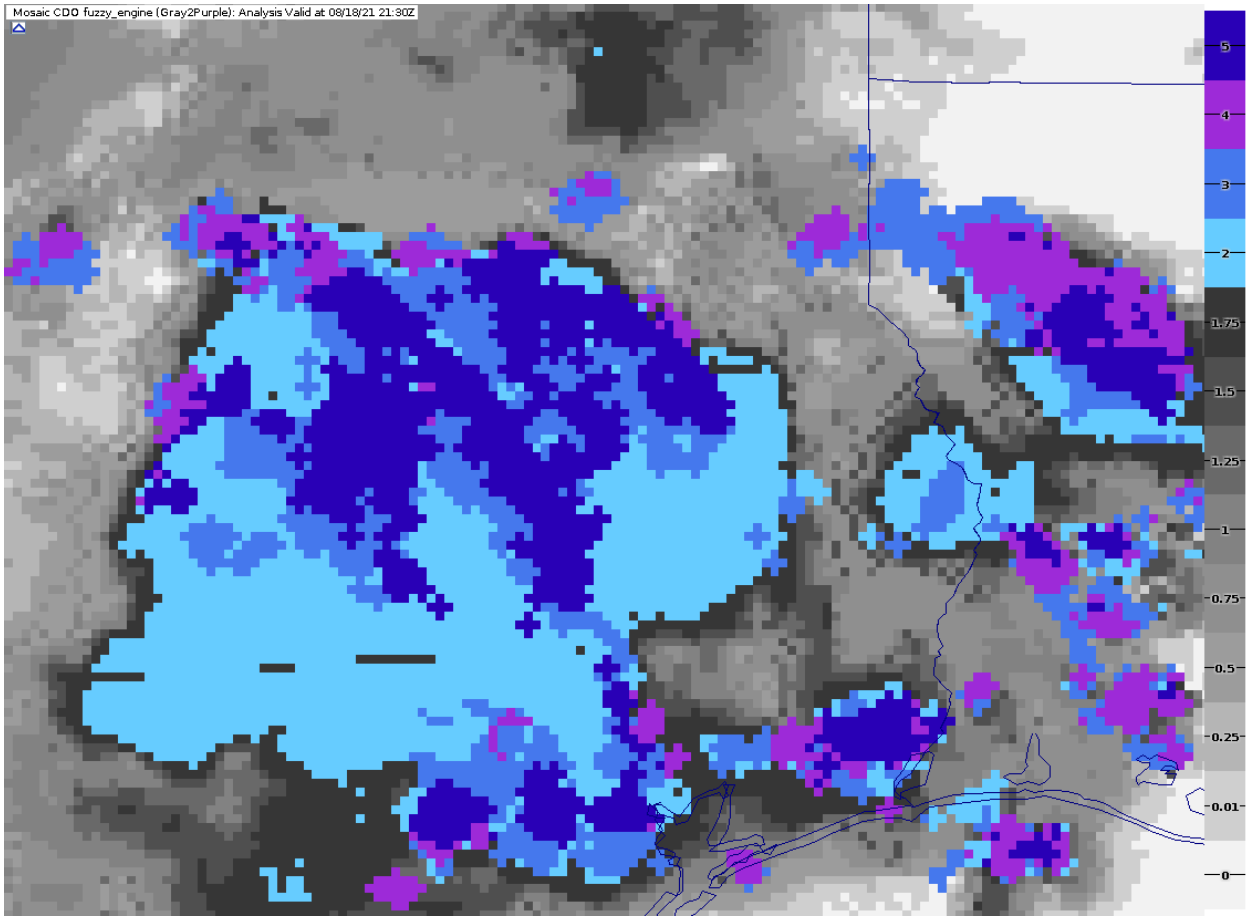

Figure 14a. The final CDO interest field computed from the four input fields. Notice that the values vary between zero and six, with values >2 indicating convective hazards are likely.

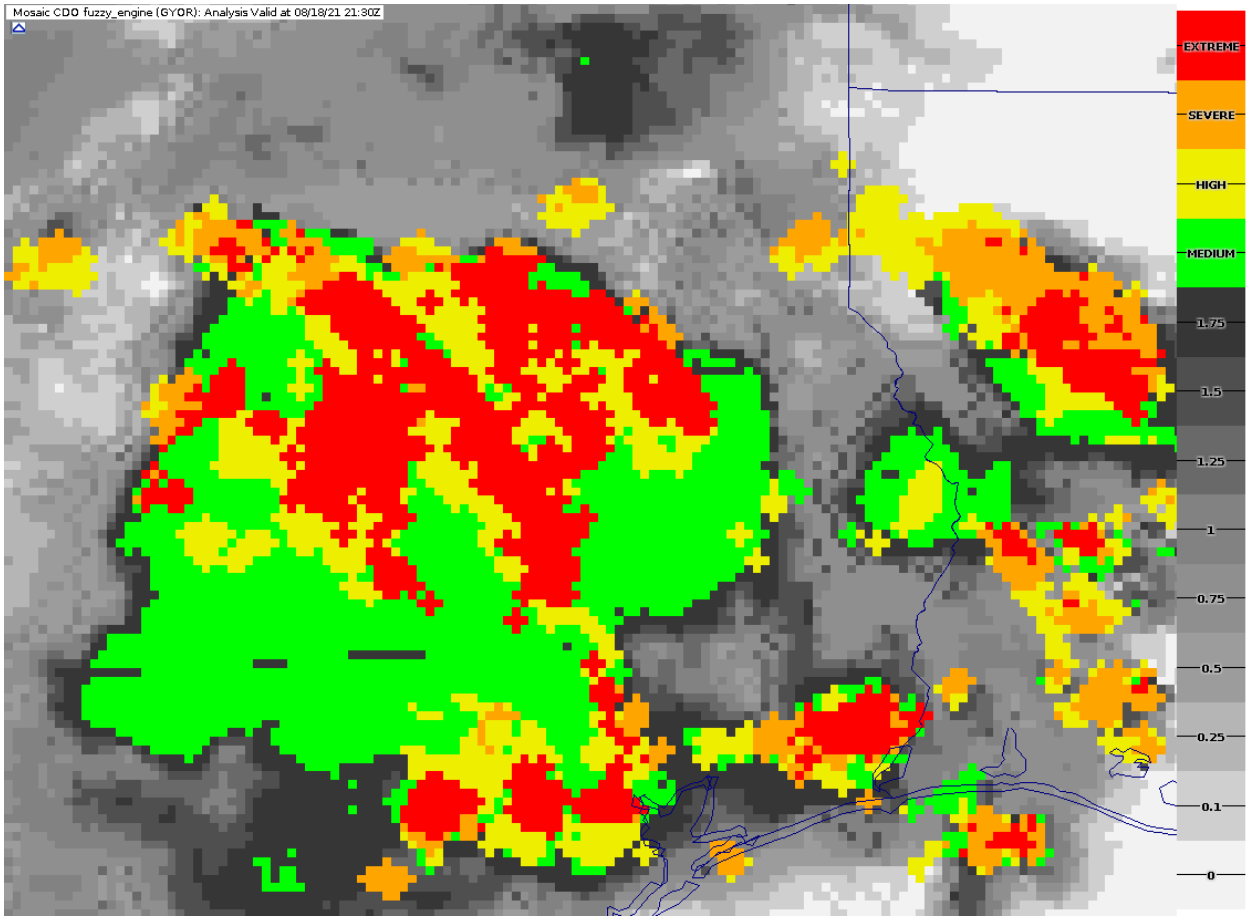

Figure 14b. Same as a), except the color scheme used by the ROMIO Viewer is shown.

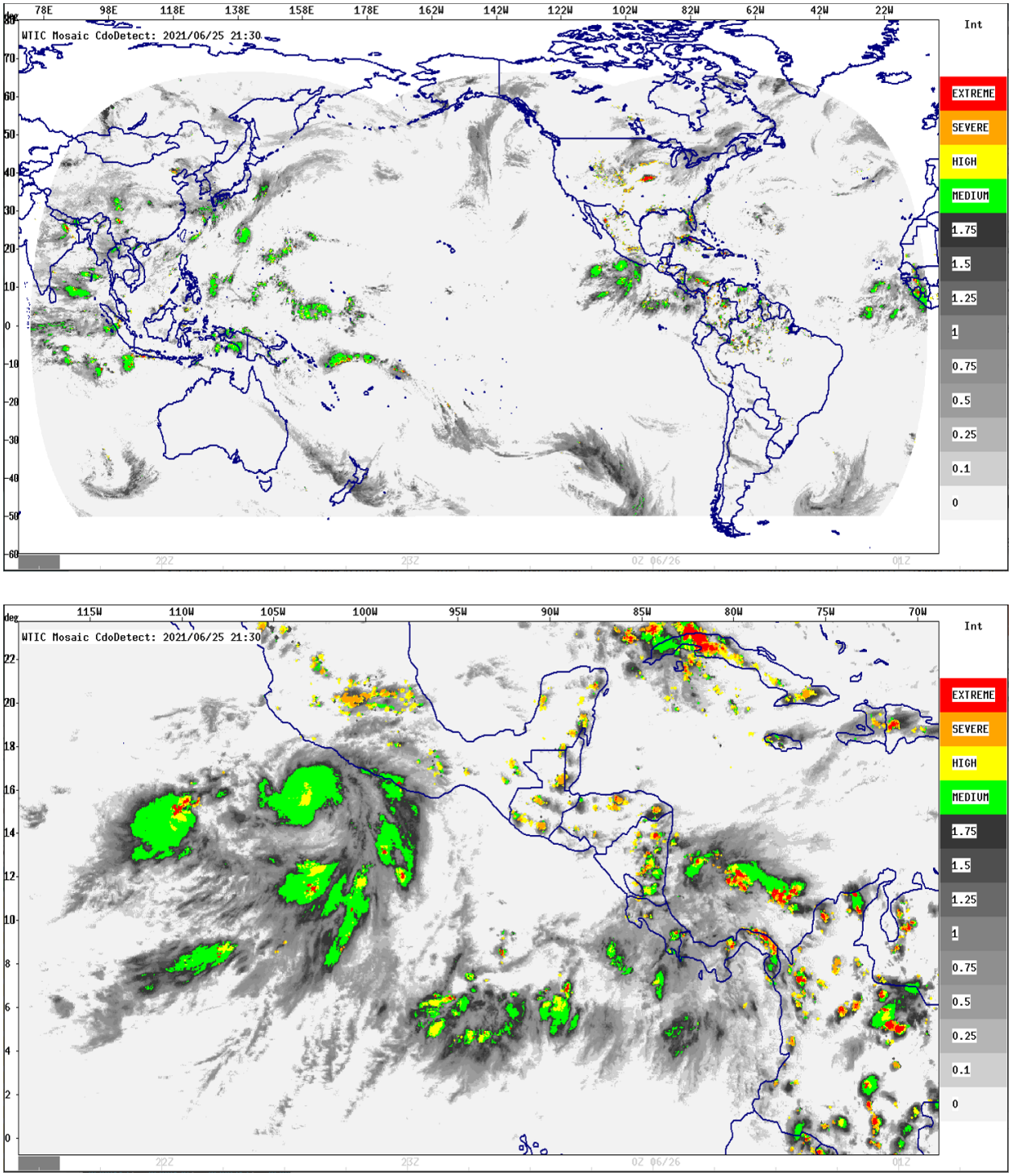

Figure 15. The CDO interest field is computed over the ROMIO domain (not for the same day as shown in Figures 13-14). The CDO is contoured such that values below 2 (i.e., not a convective threat) are contoured in shades of gray. Values at and above 2 are shaded by convective intensity. Green (CDO≥2) means "medium intensity" with no lightning, yellow (CDO≥3) means "high intensity"; orange (CDO≥4) means "severe intensity"; and red (CDO≥5) means "extreme

intensity". CDO values ≥3 mean that lighting and/or overshooting tops are present. The top panel shows CTH as computed over the entire ROMIO domain and the bottom panel shows CTH over Central America. The date is 25 June 2021 at 2130 UTC for both.

Table 2 gives a summary of several scenarios that could happen in the evolution of oceanic and or continental deep convection, typical interest values observed for CTH, GCD, OTops, the combined lightning and finally the CDO interest values.

CDO Input Interest Fields	Typical interest values for each CDO input under different scenarios					
	Growing convection w/lightning	Shallow convection w/lightning	Mature oceanic deep convection, no lightning	Mature oceanic deep convection, w/lightning	Mature continental deep convection, w/lightning and OTop	Dissipating convection
CTH (weight =1)	0.8	0.6	1	1	1	1.0
GCD (weight=1)	0.6	0.5	1	1	1	0.8
OTops (weight=1)	0	0	0	0	1	0
Combined Lightning (15, 30, 60 min) (weight=3)	3 (15+30+60)	3 (15+30+60)	0	3 (15+30+60)	3 (15+30+60)	1.5 (60)
CDO Value:	**4.4**	**4.1**	**2**	**5**	**6**	**3.3**

Table 2. Summary of various scenarios that illustrate a range of CDO interest values.

Polygon Creation

For feature identification within the gridded data for CTH and CDO, a minimum value is specified for the contour value and for the minimum storm area. For ROMIO purposes, five threshold contour values for CTH are specified (i.e., FL320, FL340, FL360, FL380 and FL400) and feature polygons are created that define each of the flight levels. Likewise, for CDO, four threshold values are specified (2, 3, 4, and 5 interest) and feature polygons are created for those interest values.

To create the feature polygons (Dixon and Wiener, 1993), a pre-set number of points (i.e., 72) are equally spaced around the compass at 5° intervals, radiating from the feature centroid. Figure 16 illustrates the process of feature identification for two storms, one larger than the other. The left panel is the full resolution CTH gridded data that are input into the contouring algorithm. The right panel shows the filled, color polygons derived from the gridded data. For each storm, a circle is drawn that encloses it and eight radials are drawn from the storm centroid (eight are shown for simplicity while the contouring algorithm uses 72). The red dots show the edge of the polygon that is defined for the FL300 contour.

These examples show that the distances between points for the larger storm is typically greater, while the distance between points for the smaller storm is less. As a result, polygons from larger storms may have a more jagged appearance than those from smaller storms. The polygons are a representation of the approximate storm contour but not an exact duplicate. Simplifying the storm contour is needed to reduce communication bandwidth needed to transmit the polygons to the flight deck.

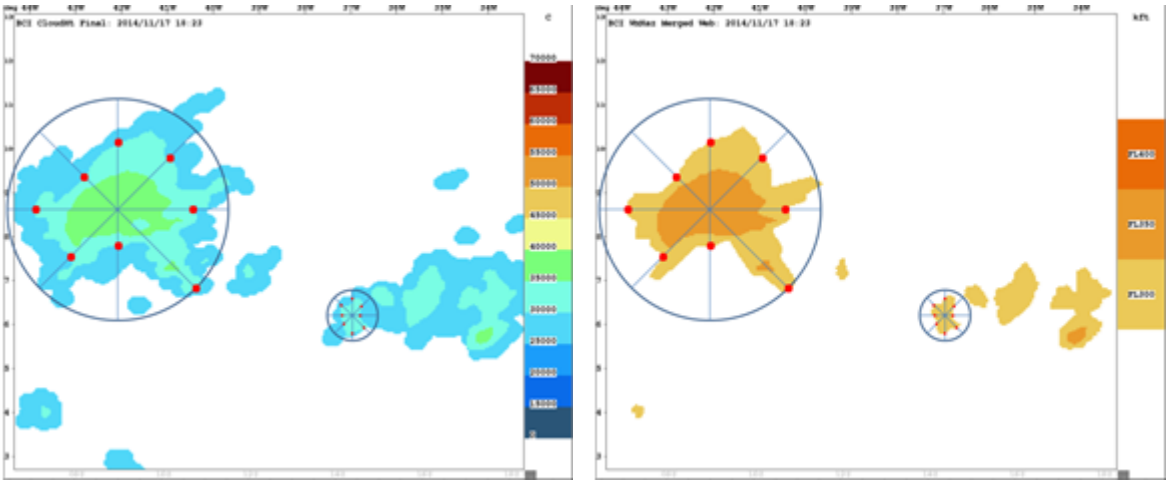

Figure 16. An example of how storm polygons are created by using points around the compass (8 points are shown instead of 72) that radiate from the feature centroid. The left panel shows the input, gridded CTH field and the right panel shows the resulting polygons (that have been filled with shading). Large polygons typically have more distance between points than small polygons and a more jagged appearance.

The polygon contours are drawn on a “greater than or equal to” basis. This means that the polygon contour for FL320 separates cloud top heights that are less than FL320 from cloud top heights that are greater than FL320. Figure 17 shows an example of how the polygon contours look in the vertical using a photo of a thunderstorm as reference. For instance, it is seen that there is considerable cloud above FL320, as also FL340 and FL360. The highest CTH value is at FL380. The contours can be considered similar to how terrain contours are drawn on a mountain.

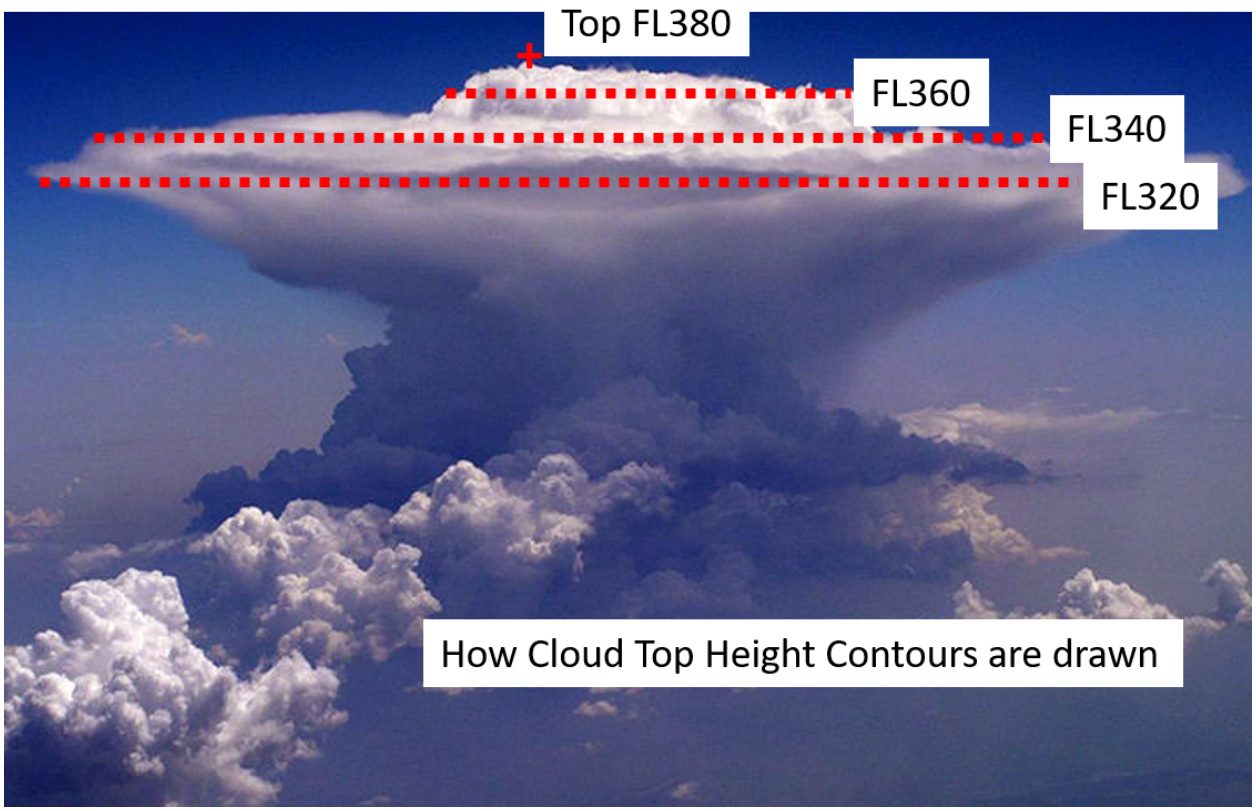

Figure 17. Conceptual CTH polygon contours are shown on this photograph of a thunderstorm to illustrate how CTH contours are drawn.

Figures 18 and 19 show examples of the CTH and CDO polygon creation, respectively. The gridded, full resolution data are shown in the left panel and the representative polygon is shown in the right panel for each. Notice the simplification of the storm shape that is achieved by the polygon. The polygons use an XML format that allows transmission of the files to the cockpit with a minimum of bandwidth use.

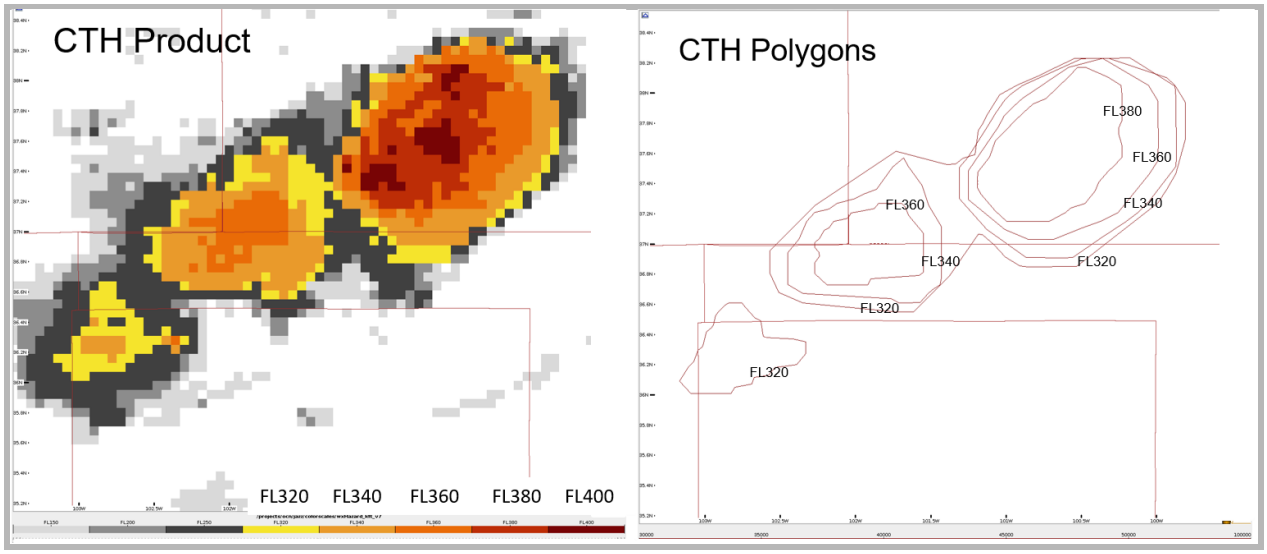

Figure 18. An example is shown of the conversion of the CTH gridded data into CTH polygons.

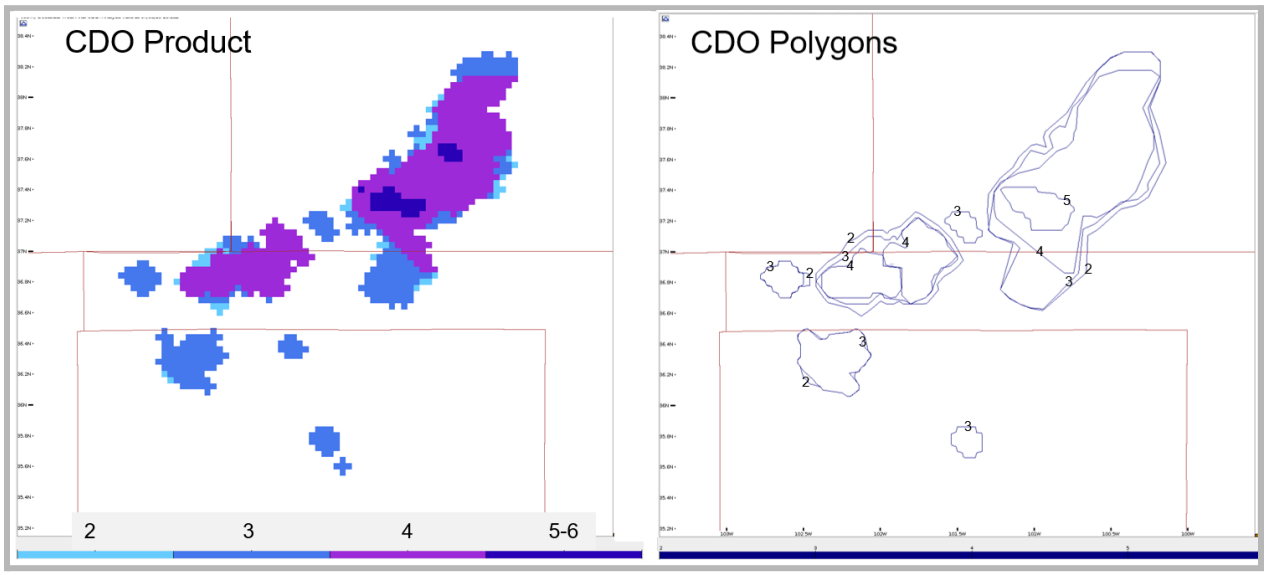

Figure 19. An example is shown of the conversion of the CDO gridded data into CDO polygons.

Maximum CTH within CDO>=3 contour

A symbolic product is generated that specifies the maximum height of the CTH product within the CDO≥3 contour. This product gives the location of that maximum height. For developing storms that may be below FL320 yet have a strong enough updraft that lightning can be produced, there will be a CDO polygon created but no CTH polygon. Having the maximum CTH within the CDO≥3 contour allows pilots to see the maximum CTH within strong storms that are below FL320. Figure 20 shows an example of this symbolic product.

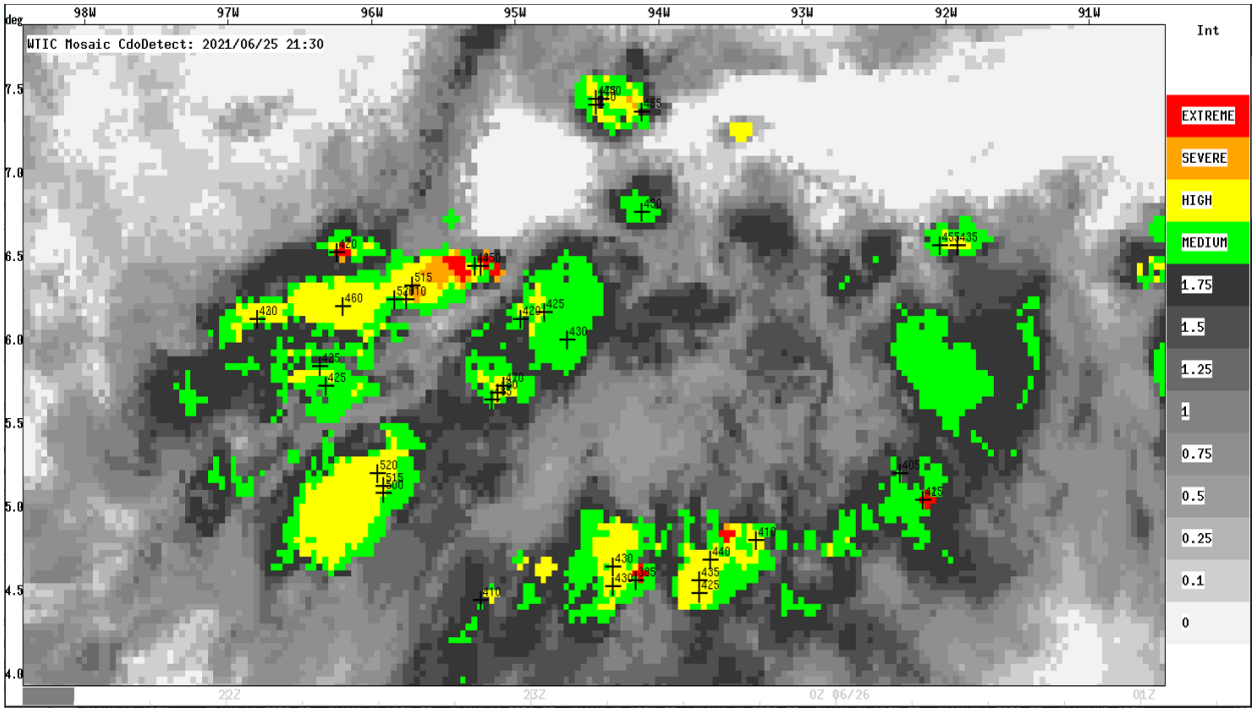

Figure 20. An example of the symbolic product (location indicated by "+") where the maximum CTH value is found within the CDO≥3.0 contour (i.e., the yellow shaded regions). The maximum CTH value is indicated to the upper right of the "+" as a flight level.

Missing data contours

In the event that input data become unavailable and either the CTH or the CDO product cannot be computed, missing data contours are provided to users.

For CTH, if the 11.2 micron channel is not available from a particular satellite, the CTH product cannot be computed and the data will be missing for that satellite. If the GFS numerical model data are not available, the CTH product will not be computed over the entire 3-satellite domain. Figure 21 shows an example of the CTH missing data contour. The polygon is continuous; however, due to limitations of the display program used, the polygon is broken at -180 deg longitude.

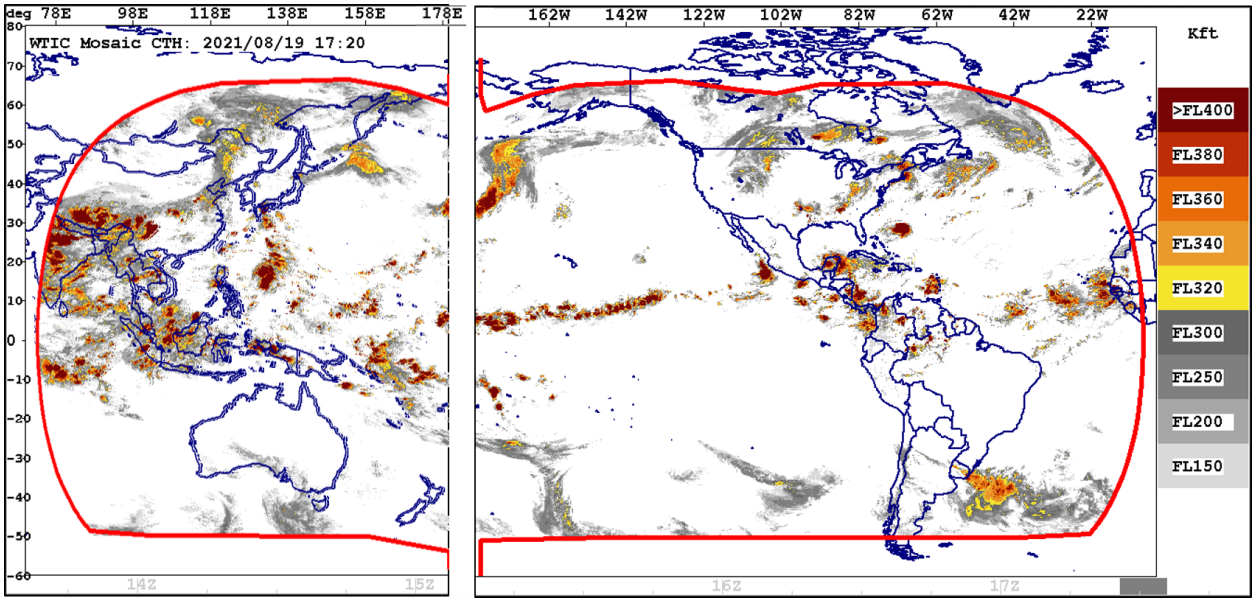

Figure 21. An example of the CTH missing data contour is shown by the red polygon.

For the CDO, the missing data contour is drawn if both satellite and lightning data are not available. If both the 6.2 and the 11.2 micron channel are not available from a particular satellite, but the lightning data are available, the CDO product will be created but it's performance will be downgraded. Figure 22 shows an example of the CTH missing data contour.The polygon is continuous; however, due to limitations of the display program used, the polygon is broken at -180 deg longitude.

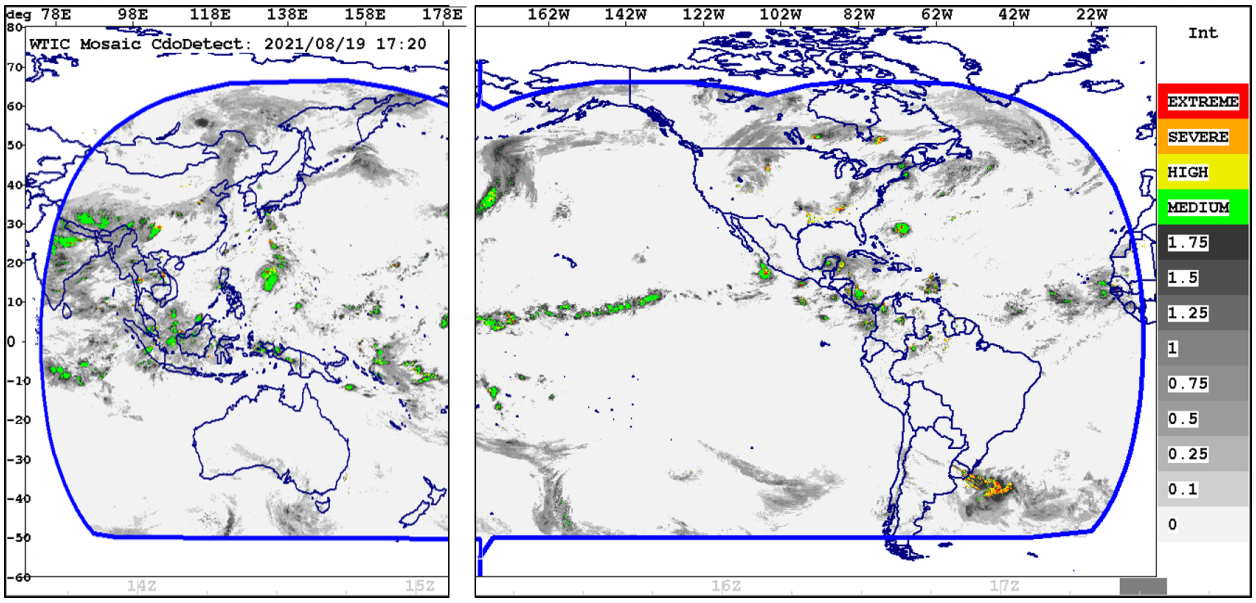

Figure 22. An example of the CDO missing data contour is shown by the blue polygon.

References

Bedka, K., J. Brunner, R. Dworak, W. Feltz, J. Otkin, T. Greenwald, 2010: Objective satellite-based detection of overshooting tops using infrared window channel brightness temperature gradients, *J. Applied Meteorology and Climatology*, **49** (2), 181-202. DOI: http://dx.doi.org/10.1175/2009JAMC2286.1

Dixon, M.J., and G.M. Wiener, 1993: TITAN: Thunderstorm identification, tracking, analysis, and nowcasting--a radar-based methodology. *Journal of Atmospheric and Oceanic Technology*, **10**, 785-797, DOI: 10.1175/1520-0426(1993)010%3C0785:TTITAA%3E2.0.CO;2.

Donovan, M.F., E.R. Williams, C.J. Kessinger, G.E. Blackburn, P.H. Herzegh, R.L. Bankert, S.D. Miller, and F.R. Mosher, 2008: The identification and verification of hazardous convective cells over oceans using visible and infrared satellite observations. *Journal of Applied Meteorology and Climatology*, **47**, 164-184, DOI: 10.1175/2007JAMC1471.1.

Donovan, M.F., E.R. Williams, C.J. Kessinger, N.A. Rehak, H. Cai, D.L. Megenhardt, R.L. Bankert, and J.D. Hawkins, 2009: An evaluation of a convection diagnosis algorithm over the Gulf of Mexico using NASA TRMM observations. *16th Conference on Satellite Meteorology and Oceanography/Fifth Annual Symposium on Future Operational Environmental Satellite Systems- NPOESS and GOES-R*, Phoenix, AZ, American Meteorological Society.

Frazier, E., C. Kessinger, T. Lindholm, R. Barron, G. Blackburn, J. Olivo, B. Watts, R. Stone, D. Keany, M. DeRis, C. Gill and A. Trani, 2018: The Remote Oceanic Meteorology Information Operational Demonstration. *2018 Integrated Communications, Navigation, Surveillance Conference (ICNS)*, Herndon, Virginia, 10-12 April 2018. DOI: 10.1109/ICNSURV.2018.8384901

Izadi, A., N. Hinze, H. Swingle, and A.A. Trani, 2019: Benefit Analysis of Remote Oceanic Meteorological Information Operational (ROMIO) Demonstration: Volume 2. Submitted to FAA WTIC Program Office, 30 September 2019, 23 pages.

Izadi, A., N. Hinze, N. Mirmohammadsadeghi, and A.A. Trani, 2020a: Benefit Analysis of Remote Oceanic Meteorological Information Operational (ROMIO) Demonstration: Volume 3. Submitted to FAA WTIC Program Office, 16 June 2020, 46 pages.

Izadi, Arman, A. Trani, M. Steiner, C. Kessinger and E. Frazier, 2020b: Benefit Analysis of Remote Oceanic Meteorology Information Operational (ROMIO) Demonstration. AIAA AVIATION 2020 FORUM. Reston, Virginia. doi:10.2514/6.2020-2912.

Kessinger, C., E. Frazier, A. Izadi, A. Trani, T. Lindholm, J. Olivo, B. Watts, R. Stone, B. Norri, S. Abelman, E. Senen, and K. Bharathan, 2020: Remote Oceanic Meteorology Information Operational (ROMIO) Demonstration, *AMS 20th ARAM Conference*, 13-16 Jan. 2020, Boston.

Kessinger, C., 2017: An update on the Convection Diagnosis Oceanic Algorithm, *18th Conf. on Aviation, Range, and Aerospace Meteorology*, American Meteorological Society, Seattle, WA, 22-26 Jan. 2017, poster 211.

Lindholm, T., C. Kessinger, G. Blackburn, and A. Gaydos, 2013: Weather Technology in the Cockpit: Transoceanic human-over-the-loop demonstration, *The Journal of Air Traffic Control*, Q1 2013, Volume 55, No. 1., 18-21.

Miller, S., T. Tsui, G. Blackburn, C. Kessinger and P. Herzegh, 2005: Technical description of the Cloud Top Height Product (CTH), the first component of the Convection Diagnosis Oceanic (CDO) Product. Submitted to the FAA AWTT Board for D3 approval, 11 March 2005, 30 pp.

Mosher, F., 2002: Detection of deep convection around the globe. *Preprints, 10th Conf. on Aviation, Range, and Aerospace Meteorology*, Portland, OR, Amer. Meteor. Soc., 289–292.

Seo, J., A. Izadi, N. Hinze, and A.A. Trani, 2019: Benefit Analysis of Remote Oceanic Meteorological Information Operational (ROMIO) Demonstration: Volume 1. Submitted to FAA WTIC Program Office, 5 August 2019, 54 pages.